MSc Mechatronic Engineering

Master Thesis

Hybrid and Fuel Cell Powertrains: two projects for small vessels

by

Carlos Fustero Martinez

s251681

October 14, 2019

30 ECTS

Supervisor:
Dr Marcello Chiaberge

Assessor:
Paolo Delzano

Politecnico di Torino

Abstract

Reducing transportation emissions is one one the biggest challenges of our society nowadays. Plug-in hybrid and electric vehicles are excellent low-emission solutions, especially if they have limited operation cycles and load profiles. When more autonomy is required, a power generation source can be added. Fuel cells are one of the most reliable and compact renewable alternatives.

The thesis covers the design and implementation of hybrid (diesel-electric) and fuel cell powertrains for two small vessels. These types of powertrains are still uncommon in the marine sector. The thesis expects to study them, test them in real projects and demonstrate if they can satisfy the project requirements. To do so, it includes a study of the principles, current state of the art, and future trends of the innovative technologies involved.

Both projects were concluded successfully, obtaining remarkable results. Technology seems to be prepared to satisfy requirements of small vessels, nevertheless, more investment is needed, especially to develop a proper hydrogen supply network.

Contents

List of Figures vi

List of Tables viii

1 Introduction 1
- 1.1 Problem statement . . . 1
- 1.2 Scope . . . 1
- 1.3 Thesis Outline . . . 2

2 Hybrid & Electric vessels 3
- 2.1 Context: Marine emissions . . . 3
- 2.2 Propulsion architectures . . . 4
  - 2.2.1 Conventional . . . 4
  - 2.2.2 Electric . . . 4
  - 2.2.3 Hybrid . . . 5
    - Series hybrid . . . 5
    - Parallel hybrid . . . 6
    - Parallel vs Series . . . 7
  - 2.2.4 Hybrid & Electric advantages . . . 7
- 2.3 State of the art . . . 8
  - 2.3.1 Nemo H2 . . . 8
  - 2.3.2 XeroPoint hybrid propulsion tugboats . . . 9
  - 2.3.3 Electrovaya electric cable ferry . . . 10

3 Projects 12
- 3.1 Projects description . . . 12
  - Projects motivations . . . 13
  - Outside the scope . . . 13
- 3.2 Operating conditions . . . 13
- 3.3 Methodology . . . 14
- 3.4 Client requirements . . . 16
  - Hybrid project . . . 16
  - Fuel cell project . . . 16
- 3.5 Engineering requirements . . . 16
  - Hybrid project . . . 17
  - FC project . . . 18

3.6 Projects architecture . . . 20
Hybrid project . . . 20
FC project . . . 21

4 Power sources **24**
4.1 Diesel engine . . . 24
4.1.1 Hybrid concept . . . 24
4.1.2 Diesel & electric limit . . . 26
4.1.3 Electric recharging torque . . . 27
4.2 Fuel cell . . . 29
4.2.1 State of the the art . . . 30
Proton exchange membrane fuel cell (PEMFC) . . . 31
Challenges . . . 32
4.2.2 Thermodynamics . . . 34
4.2.3 Polarization curve . . . 37
4.2.4 Fuel cell selection . . . 39
4.2.5 Heat Management . . . 40
Operating temperature . . . 40
Heat calculation . . . 40
4.2.6 Flow rates . . . 42
4.2.7 Cathode side . . . 43
Oxidant flow . . . 44
Cathode pressure . . . 44
Compressor . . . 45
4.2.8 Anode side . . . 46
Fuel supply . . . 46
Fuel consumption . . . 47
Fuel storage . . . 47
4.2.9 Water Management . . . 48
Cathode . . . 49
Anode . . . 49
4.2.10 DC/DC converter . . . 50
4.2.11 Efficiencies . . . 51
4.2.12 Fuel cell system . . . 53

5 Electrical components **56**
5.1 Batteries . . . 56
5.1.1 Batteries in the automotive sector . . . 56
Lead-Acid batteries . . . 56
Nickel based batteries . . . 57
Lithium-ion batteries . . . 57
5.1.2 State of the art of lithium-ion batteries . . . 57
Working principle . . . 57

Anode materials . . . 58
Cathode materials . . . 59
Electrolite materials . . . 59
Examples on the market . . . 60
Future trends . . . 61
5.1.3 Performance and degradation . . . 61
5.1.4 Selection . . . 64
Hybrid project . . . 65
FC project . . . 66
5.2 Electric motors . . . 68
5.2.1 State of the art . . . 68
5.2.2 Selection . . . 70
Hybrid project . . . 70
FC project . . . 71

6 Thermal design **73**
6.1 Heat estimation . . . 73
6.2 Cooling systems . . . 74
6.3 Hybrid project . . . 75
6.4 FC project . . . 75
6.4.1 Standard cooling system . . . 76
6.4.2 Fuel cell cooling system . . . 79

7 Hardware & Software **81**
7.1 Hardware . . . 81
7.1.1 Electronic control unit(ECU) . . . 81
Inputs: Sensors and control keys . . . 82
7.1.2 Hybrid project . . . 84
ECU . . . 84
Input pins . . . 84
Output pins . . . 85
7.1.3 Fuel cell project . . . 85
Input pins . . . 86
Output pins . . . 86
7.2 Communication networks . . . 87
7.2.1 Controller Area Network (CAN) . . . 87
7.2.2 Networks implemented . . . 90
Hybrid project . . . 90
FC project . . . 90
7.3 Software . . . 91
7.3.1 Codesys . . . 91
7.3.2 Software development . . . 91

8 Conclusion & future work **93**

8.1 Current state of the projects 93

8.2 Conclusions 93

8.3 Future work 94

Bibliography **95**

List of Figures

2.1 IMO marine emissions prediction [1] . . . 3
2.2 Electric architecture [2] . . . 5
2.3 Series hybrid architecture [3] . . . 6
2.4 Series hybrid architecture [3] . . . 6
2.5 Nemo H2 [4] . . . 9
2.6 Xeropoint architecture [5] . . . 9
2.7 Carolyn Dorothy [6] . . . 10
2.8 Electrovaya Electric Cable Ferry [7] . . . 11

3.1 Operating route . . . 13
3.2 Speed limits [8] . . . 14
3.3 V-model [9] . . . 15
3.4 Thermal efficiencies for small-medium engines [10] . . . 17
3.5 Architecture hybrid project . . . 20
3.6 Detailed scheme hybrid project . . . 21
3.7 Architecture FC project . . . 22
3.8 Detailed scheme FC project . . . 22

4.1 SFC plot [3] . . . 25
4.2 Propeller power plot [3] . . . 25
4.3 Electric torque effect on engine performance [11] . . . 26
4.4 Charging parameters . . . 28
4.5 Fuel cell performance [12] . . . 29
4.6 PEMFC cell structure [13] . . . 31
4.7 PEMFC stack [14] . . . 32
4.8 Ideal fuel cell efficiency (using $\Delta H_{H_2O_{(l)}}$) vs carnot efficiency (with an exhaust temperature of 90°) [15] . . . 35
4.9 Nernst voltage with respect to temperature in a hydrogen/oxygen PEMFC at 1 atm [15] . . . 36
4.10 Polarization curve [15] . . . 37
4.11 PEMFC losses [15] . . . 38
4.12 Stack polarization curve . . . 39
4.13 Close field vs Open field . . . 39
4.14 Temperature effect on PEMFC polarization curves [16] . . . 40
4.15 Fuel cell energy balance [17] . . . 41

4.16 Heat generation of the fuel cell . . . 42
4.17 Cathode side . . . 43
4.18 Cathode air flow & stoichiometric ratio . . . 44
4.19 Input cathode pressure . . . 44
4.20 Compressor pressure ratio vs flow . . . 45
4.21 Compressor power consumption vs flow . . . 45
4.22 Anode side . . . 46
4.23 Fuel consumption . . . 47
4.24 Water management [18] . . . 48
4.25 Fuel cell efficiencies (liquid water) . . . 52
4.26 Fuel cell efficiencies (vapor) . . . 52
4.27 Fuel cell system scheme . . . 53
4.28 Fuel cell system photo 1 . . . 55
4.29 Fuel cell system photo 2 . . . 55

5.1 Lithium battery performance [19] . . . 58
5.2 Future trends of lithium ion batteries [19] . . . 61
5.3 Generic lithium ion battery charging curve [20] . . . 62
5.4 Current effect on generic lithium ion battery [20] . . . 62
5.5 Temperature effect on generic lithium ion battery [20] . . . 62
5.6 Lithium ion battery degradation [21] . . . 63
5.7 Batteries operating parameters and degradation [22] . . . 64
5.8 Generic BMS [23] . . . 64
5.9 Discharge profile hybrid project . . . 65
5.10 Discharge profile FC project . . . 67
5.11 Efficiency PM synchronous(left) vs induction(right)[24] . . . 68
5.12 Generic inverters efficiency vs load[25] . . . 70
5.13 Hybrid project motor mounted . . . 72
5.14 FC project inverters and motor during tests . . . 72

6.1 Standard cooling system . . . 76
6.2 Internal pumps FC project . . . 78
6.3 External pumps FC project (LCB 20/E) . . . 78
6.4 Fuel cell cooling system . . . 79

7.1 ECU scheme . . . 81
7.2 ECU hybrid project . . . 84
7.3 ECU FC project . . . 85
7.4 CAN scheme [26] . . . 87
7.5 Weight reduction CAN [27] . . . 87
7.6 CAN voltage levels [28] . . . 88
7.7 CAN comunication [29] . . . 88
7.8 CAN arbitration [29] . . . 89

List of Tables

4.1 Diesel engine characteristics 24
4.2 Fuel cell types [30] 30
4.3 Free energy of Gibbs vs temperature [31] 35
4.4 Heating values vs temperature 41
4.5 Hydrogen storage 47
4.6 DC/DC operating conditions 50
4.7 DC/DC technical characteristics 50
4.8 Fuel cell system operation points 53
4.9 Fuel cell system efficiencies 54

5.1 Lithium ion batteries: anode materials [19] 59
5.2 Lithium ion batteries: cathode materials [19] 59
5.3 Lithium batteries in the automotive sector [32] 60
5.4 Battery set hybrid project 65
5.5 Battery set FC project 66
5.6 State of the art of electric motors 69
5.7 Electric motor & inverter hybrid project 70
5.8 Electric motor & inverter FC project 71

6.1 Water and ethanol glycol combination 74

7.1 Inputs hybrid project 84
7.2 Outputs hybrid project 85
7.3 Inputs FC project 86
7.4 Outputs FC project 86

Chapter 1

Introduction

The transportation sector uses around 25% of the worldwide commercial energy and its emissions are constantly growing [4]. Environmental concern has increased and legislation is forcing technology to develop new solutions for this global challenge.

Hybrid, electric and fuel cell vehicles appeared as one of the most promising technologies to reduce emissions and fuel consumption. There are already plenty of models in the market and these technologies, boosted by legislation and current investments, may achieve mass-market penetration in the next decades. However, more research is needed, especially to extend these technologies beyond the road vehicles.

1.1 Problem statement

In Venice, possible future limitations on diesel vessels within the city center are forcing companies to find new transportation alternatives.This motivated a private company in charge of public transportation service to develop two new green models for their fleet, a hybrid (diesel-electric) and a fuel cell one. The challenge consisted in designing and implementing a hybrid and a fuel cell powertrain in two of their conventional models. Each project has different performance requirements.

The projects were carried out by Dolomitech, a different company specialized in designing and implementing hybrid, electric and fuel cell powertrains. As a Dolomitech employee, I had the chance to join the project group, composed of 4 members, responsible for both projects.

1.2 Scope

Hybrid and fuel cell automobiles have attracted public attention in the last decades, however, these powertrains are still uncommon in the marine sector. Focusing on small vessels, this thesis expects to study these technologies, test them in real projects and demonstrate if they can satisfy the project requirements.

Therefore, the thesis covers the design and implementation of both powertrains for two small vessels. To do so, it includes a study of the principles, current state of the art, and future trends of the innovative technologies involved. The internal control of the different components is generally carried out by the suppliers (excluding the fuel cell) and the main tasks are:

- Choose the project architecture
- Translate client requirements into engineering ones
- Select, control, and integrate the different components

1.3 Thesis Outline

The thesis is structured as follows:

- Chapter 2: Introduction to hybrid and electric powertrains and examples of current projects.
- Chapter 3: Project description, methodology, client requirements, engineering requirements and architectures.
- Chapter 4: Power sources (diesel engine and fuel cell system).
- Chapter 5: Main electrical components (high voltage batteries and electric motors).
- Chapter 6: Thermal design (cooling systems).
- Chapter 7: Hardware and Software.
- Chapter 8: Current state of the projects, conclusions and future work.

Chapter 2

Hybrid & Electric vessels

2.1 Context: Marine emissions

The marine sector emissions represent more than 30% of the CO_2 transportation sector emissions and between a 3% to 4% of the global anthropogenic emissions [4]. The percentage is even greater in terms of NOx and SOx emissions, with approximately 37% and 28% respectively [1].

The International Marine Organization (IMO) is one of the main international institutions in the sector and its regulations have a worldwide scope. The IMO realized a study to predict the expected increase of CO2 emissions in the marine sector. Different scenarios were proposed, predicting the most probable ones and the limit scenarios annual increments between 1.9%-2.7% and 0.8%-5.2% respectively [1].

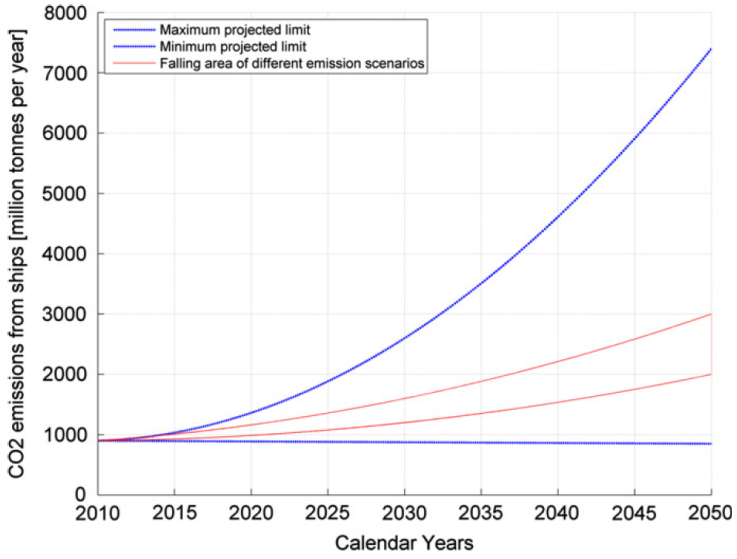

FIGURE 2.1: IMO marine emissions prediction [1]

According to the study, if the marine sector does not stabilize its emissions, in 2050 marine emissions will reach values between 12%-18% of the global permissible CO2 emissions[1].

2.2 Propulsion architectures

To remain inside the scope of the project, only the propulsion architectures for small vessels (less than 24m length) are discussed. These vessels are generally characterized by demand profiles with high speed transients and short operating cycles.

2.2.1 Conventional

The typical architecture consists of a gas or diesel engine and a propeller that is directly driven through a gearbox. Part of the mechanical energy produced is transformed into electrical energy through an alternator. This energy is used to charge a battery and feed all the electric loads.

In the last decades, modern engines have been highly optimized in their operating designed ranges and have reached high efficiencies. However, their efficiency significantly decreases out of these ranges, increasing their emissions and fuel consumption. In ships, more engines can be added in order to have more degrees of freedom and keep operating efficiently. Unfortunately, this cannot be applied for small vessels with only one engine, which is frequently used inefficiently.

2.2.2 Electric

The concept of this architecture is simple; a source provides energy to the electric motor that drives the propeller. Different sources could provide energy; some of the most promising ones involve renewable sources, fuel cells or battery packs. Nevertheless, renewable energies depend on unreliable sources (wind, sun, etc...) and fuel cells may have problems to satisfy peak power demands.

Renewable electric sources are generally combined with an energy storage system (flywheels, supercapacitor, batteries, etc..). Supercapacitors and flywheels are generally used to cover those power peaks while batteries, due to their higher energy density, can also be used alone to power short-medium range operation vessels. As an example, figure 2.2 schematically represents an architecture based on the combination of a fuel cell and a battery energy storage system.

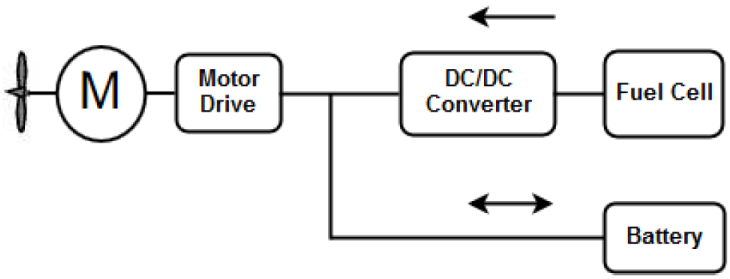

FIGURE 2.2: Electric architecture [2]

The challenge of this technology relays on the capacity to meet both power and energy requirements. Despite its recent development, it still imposes important constraints in terms of performance (mainly autonomy) and cost.

Electric propulsion is especially suitable for short-medium range and relative low-speed vessels. Some possible applications could be sailboats, passenger boats or yachts. Economically viable projects have been proved such as the canal Nemo H2 in Amsterdam or all-electric ferries in Norway [3].

2.2.3 Hybrid

This architecture combines elements from both previous ones as it integrates conventional engine technology with these new high-performance components. An internal combustion engine (ICE), an electric storage unit and an electric motor are the main components of a hybrid architecture.

Hybrid systems are based on the combination of different energy sources to satisfy the vessel power and energy demands. The vessel can be driven by the electric storage unit and the electric motor or directly by the engine. The idea is to use the energy storage system to limit the ICE operation to its efficient region. The main hybrid configurations are series, parallel or a combination of both.

Series hybrid

The combustion engine and the electrical system are connected in series to the propeller (figure 2.3). The internal combustion engine is connected to a generator that provides energy to the electrical system. The electrical system drives the propeller through an electric motor and uses the electrical storage system to decouple power production and consumption.

To sum up, the engine produces electricity in its most efficient region and the difference between its production and the motor consumption compensated by the electrical storage system. The more sets of generators and storage systems, the more flexibility to optimize the different operating points. Unfortunately, small boats are strongly limited in terms of mass and space. It is important to highlight that it is not a diesel-electric system as there is an electric storage system in this architecture.

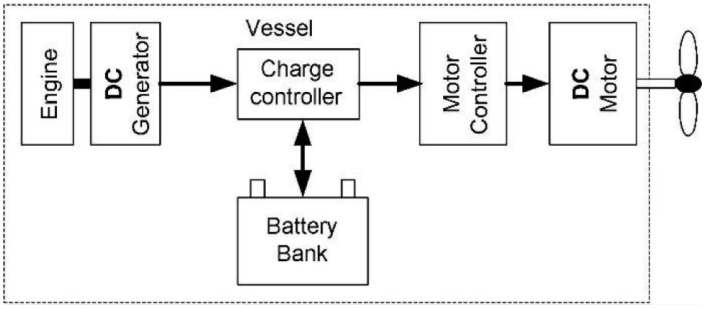

FIGURE 2.3: Series hybrid architecture [3]

Parallel hybrid

In this configuration, the engine and the electrical system are connected in parallel to the propeller and both can power it (figure 2.4). Both are mechanically coupled and connected to the same shaft through a gearbox or a cluster. The electric machine now can act as a motor to drive the propeller or as a generator applying a load to the shaft and charging the storage system.

In general, the electric motor and the ICE drive the vessel in different speed ranges. ICE efficiency decreases significantly when operating at reduced loads, so the electric motor drives the vessel at low speeds. Additionally, it can be used combined with the engine to increase the maximum power during transients. The ICE drives the vessel at high speeds (where its efficiency is higher) and charges the storage system.

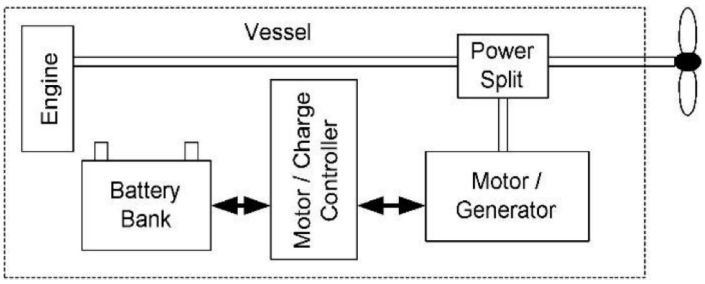

FIGURE 2.4: Series hybrid architecture [3]

Parallel vs Series

Compared to the series configuration, the parallel one offers:

- Lower number of components
- Smaller electric motor
  In the series configuration, the electric motor must manage the peak loads.
- Fewer batteries required
- Fewer losses due to energy conversion
- More reliability and redundancy
  If the electrical system or the engine suffers problems, the other one can still power the vessel.

Series configuration is restricted to concrete applications, for example, vessels with a high proportion of house loads. One of its advantages consists of the absence of a mechanical link between the propeller and the engine. This allows locating them in different zones achieving a better distribution of the space.

2.2.4 Hybrid & Electric advantages

Compared to conventional propulsion, the main advantages offered by electric and hybrid configurations are summarized in the following list [4, 3]:

- Emissions and water pollution reduction
  Depending on the power source, electric vessels can operate with zero emissions. Hybrid ones can reduce them significantly.
- Fuel savings (possible economical boost)
- Better manoeuvrability
- Noise and vibrations reduction
  The comfort improvement is one of the main attractions for the user.
- 'Being green' image

Electric and series hybrid configuration also offer:

- Flatter torque curve in electric motors.
  Electric motors have plenty of torque available at every speed, which allows the use of high efficient propellers. They can offer an overall improvement of efficiency of 15-25% compared to the conventional ones.

- More degree of freedom in naval architecture in electric propulsion
  There is no mechanical link between the propeller and the engine.

Parallel hybrid configuration also offers:

- Increase of reliability and redundancy

These advantages are boosted when vessels have operating cycles that do not match the efficient regions of conventional engines. On the other hand, the main challenges to solve are [4, 3]:

- Increase of financial costs and initial investment.

- Losses in energy conversion and storage and the consequently loss of system efficiency.

- Lack of qualified technicians and replacements for maintenance and reparation works.

- Lack of suppliers of hydrogen in case of systems with fuel cell.

2.3 State of the art

2.3.1 Nemo H2

Presented in Amsterdam in 2009, it is one of the first fuel cell vessels. It is a passenger boat with 22 meters length and 4 meters width, able to transport up to 86 passengers. A 60 kW PEMFC fuel cell system and a 70kWh lead- acid battery set drive the vessel [4]. The battery set provides extra power when needed and it is charged when the vessel does not operate with high loads.

FIGURE 2.5: Nemo H2 [4]

2.3.2 XeroPoint hybrid propulsion tugboats

Aspin Kemp Associates (AKA) has recently developed the XeroPoint hybrid propulsion system. As it is shown in figure 2.6, it consists of a diesel engine and an electric motor that can power simultaneously or independently the propulsion shaft. Both of them are commanded to meet the vessel demands optimizing the engine operation point and adding redundancy to the system.

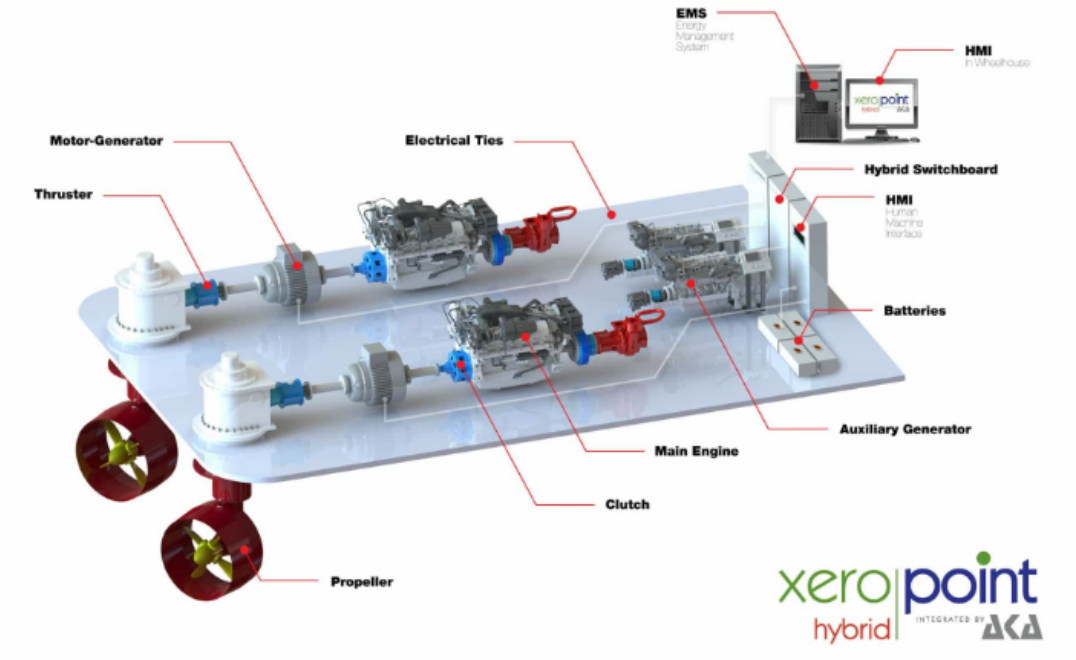

FIGURE 2.6: Xeropoint architecture [5]

In 2009 it was carried out the first implementation of this propulsion system, the FOSS Green Assist^{TM} vessel called Carolyn Dorothy. This dolphin class tug became the world's first hybrid tugboat with its 670 horsepower.In 2010 the UC Riverside College of Engineering and the Center for Environmental Research and Technology (CE-CERT) conclude a study about its fuel savings and emissions reduction. Fuel savings between 20-30% were achieved and even greater emission reductions. PM, NOx, and CO2 emissions were decreased by a 73%, 51% and 27% respectively [33].

FIGURE 2.7: Carolyn Dorothy [6]

After the success of this initial project, the propulsion system was used in more tug projects. In 2011 RT Adrian started operating in the Rotterdam port, becoming the first European hybrid tug.

2.3.3 Electrovaya electric cable ferry

This ferry, able to carry 49 passengers and 6 cars, realizes 10 round-trips of 1.6Km per day, between the mainland and the Hisarøy Island. The propulsion is supplied by lithium ion batteries that are charged on the mainland between trips and at night. During its whole life cycle is could save 180,750 liters of fuel, 480 tones of CO2, 9 tones of particulate matter and volatile organic compounds, 2 tones of carbon monoxide and 2 tones of other types of emissions [7].

FIGURE 2.8: Electrovaya Electric Cable Ferry [7]

Chapter 3

Projects

3.1 Projects description

A company in charge of the public transportation service in Venezia decided to develop two new green models, a hybrid (diesel-electric) and a fuel cell electric vessel. For simplicity, they are called hybrid and fuel cell project respectively, even if both models could be considered hybrid as the fuel cell one includes a battery set. Their idea was to develop new powertrains for one of their current vessel models. The existing model used in both projects has a length and width of 15 and 4 meters respectively and can carry up to 40 passengers. Both vessels are prototypes and just one unit of each has been initially constructed.

Hybrid project

It is expected to operate as an electric boat within the city and as a diesel vessel outside it. Actually, at low speeds it is electrically powered without contaminating and over a certain speed demanded, the diesel engine starts powering the vessel. During the diesel mode, electrical energy is stored in the batteries., This energy is later used to operate the vessel in electric mode. Furthermore, a plug-in interface allows charging the batteries at night or when the vessel is not working.

Fuel cell project

It is completely electric and has zero emissions while operating. The vessel is driven by the combination of a fuel cell and a battery set. The vessel is mainly driven by the batteries, the fuel cell generates constant power to increase their autonomy and charge them during low power demands. Even if the fuel cell is off, the batteries can drive the propeller alone. It also has a plug-in interface that allows charging the batteries at night or when it is not operating.

Projects motivations

New legislation constrains suppose an important incentive for renewable projects. Air and water contamination concern is increasing in Venice and the town hall is planning to impose new limits on diesel vessels within the city center. According to our client, transportation companies will soon be forced to renew their fleets as in the future only electric vessels may be able to operate within the city center. Public funds promoting renewable projects and the company image improvement were also relevant motivating factors.

Outside the scope

In the hybrid model, the diesel engine the gearboxes are not part of the Dolomitech project. The diesel internal control is out of the thesis scope, however, it is commanded by the Dolomitech electronic control unit (ECU).

3.2 Operating conditions

The client operates different lines in Venezia, which connect the city with both airports. In our case, both vessels are design to operate the same line, which is represented in figure 3.1 and has the largest path inside the city. The hybrid model may also operate other lines if it has to recharge its batteries.

FIGURE 3.1: Operating route

Different speed limits are imposed depending on the sailing area. The speed limits within the city are 5, 7 or 11 km/h and 20 km/h outside it. A speed limit map is shown in figure 3.2.

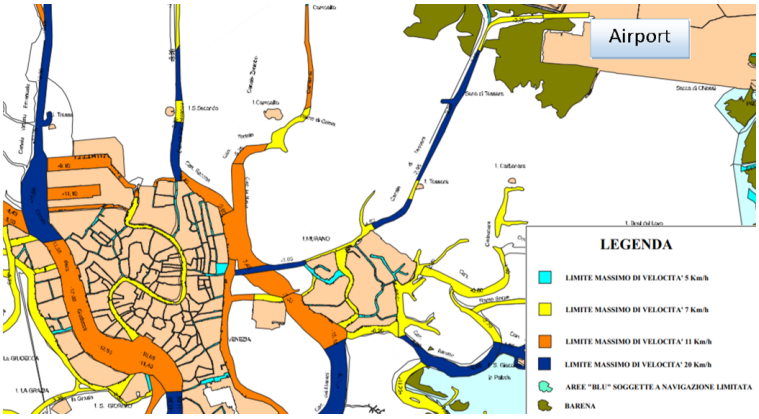

FIGURE 3.2: Speed limits [8]

With a total path of 11.6 km, the route is characterized by:

- 3.2 km with a speed limit of 20km/h (high-speed section)
- 1.8 km with a speed limit of 11km/h (medium-speed section)
- 6,6 km with a speed limit of 5km/h or 7 km/h (low-speed section)

The high, medium and low-speed regions represent 27.5%, 15.5% and 53% of the total path respectively. Low-speed regions are dominant and they are not only located in the city (the airport entrance contributes with 2,3 km). According to their published timetables, it takes approximately 75 minutes to complete the whole route. Additionally, it remains 15 and 30 minutes at the airport and last city stop respectively.

3.3 Methodology

Dolomitech followed the V-model to properly manage the project from conception to retirement. It is a linear development methodology in which requirements drive the design and testing to achieve cost effectiveness and client satisfaction. The following stages are followed:

1. Client requirements
   Though several meeting with the client, the operation requirements are written in a formal document.

2. Engineering requirements
   Client requirements are translated into engineering ones allowing Dolomitech to start designing the project.

3. Project architecture
   The system architecture is defined.

4. Detail design
   The main subsystems are studied and designed. It includes aspects in which the thesis does not focus on, such as the system electric circuits or the auxiliary mechanical pieces required to fix the components

5. Implementation

6. Unit testing
   Basic tests were carried out in the acquired components as they have already been characterized by the suppliers. Mainly software, cooling systems, CAN networks and fuel cell system were tested. The tests ensured that behavior and communications were correct and that requirements were achieved.

7. System testing
   The system behavior was tested. The focus was on the global software behavior as it is in charge of the performance.

8. Operation and maintenance
   As both model are prototypes, the model are continuously optimized according to the operational feedback.

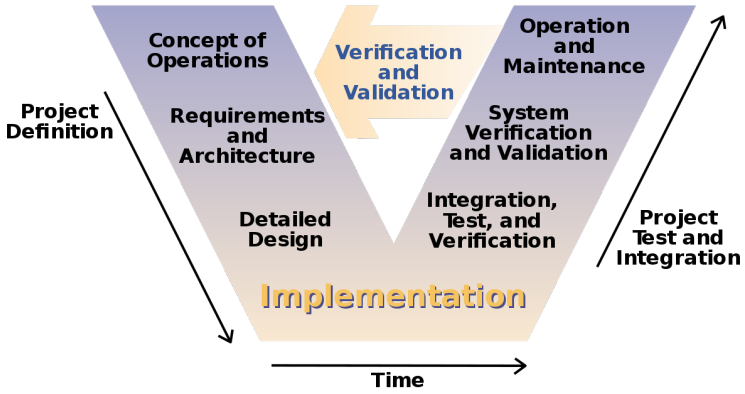

FIGURE 3.3: V-model [9]

3.4 Client requirements

Hybrid project

The vessel is only electrically powered at low speeds. The client expects the electric power train to provide enough power to continuously hold a maximum speed of 7-8 knots (13-15 km/h) in standard climate conditions.

In terms of autonomy, the vessel must be able to store enough energy to power the vessel for 60 minutes. A power consumption equal to 50% of its maximum power is considered.

Fuel cell project

The maximum power must be equal to the maximum output power of the conventional models, or in other words, it must be around 170kW. This output power is only guaranteed when the batteries are charged, otherwise, it is limited to the one produced by the fuel cell. In this case, the performance is expected to be reduced, however, the vessel must be able to move and reach a safe point where it can be charged. This power mode is not desired and its use should be exceptional.

In terms of autonomy, the vessel must be able to complete a journey, considering the batteries charged and hydrogen tanks full. This implies sailing around 10h a day.

3.5 Engineering requirements

The client requirements were translated into engineering requirements to design both power trains. The main parameters to establish are the maximum power and capacity. To estimate them, both projects take advantage of the fact that fuel consumption can be measured in conventional models. It is not necessary to be extremely precise on the estimations as a security margin is applied when selecting components.

The efficiency of conventional models must be known to obtain useful information about those measurements. Unfortunately, no engine technical data could be provided by the client so its efficiency had to be estimated. The thermal efficiency of an engine is defined as the output power divided by the input thermal energy. In figure 3.4, the peak thermal energy of different small to medium-sized engines is shown.

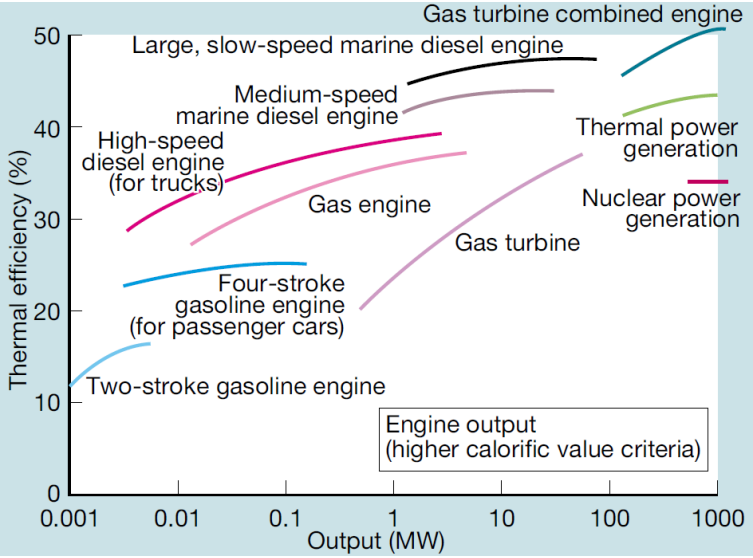

FIGURE 3.4: Thermal efficiencies for small-medium engines [10]

The client uses high-speed engines with an output power of 0.17 MW. The peak efficiency of the system is estimated around 35%, nonetheless, efficiency highly depends on the load. According to the diesel operating conditions, different efficiencies were considered.

Hybrid project

Power requirements

The maximum electrical power was estimated applying the following procedure:

1. Measure fuel consumption
   The fuel consumption measured in a conventional model was around 11 l/h with a speed around 7-8 knots in standard climate conditions.

2. Estimate the diesel system efficiency
   The engine load was around 20% of its maximum load (170kW). Under these conditions, the engine efficiency should be approximately half of its maximum efficiency. A 20% efficiency is considered.

3. Calculate the mechanical power required
   Considering that every diesel liter contains approximately 10kWh of thermal energy, the mechanical power required is equal to

$$P_m = \text{fuel consumption(l/h)} \cdot \text{diesel thermal energy (kWh)} \cdot \eta_{diesel} = 22kW$$

4. Calculate the electrical power required

   The electrical efficiency must be applied to obtain the electrical power required. High efficient motors and controllers are used and an 80% efficiency was conservatively considered at high loads.

   $$P_{elec} = \frac{P_m}{\eta_{elec}} = 27.5kW \approx 30kW$$

   For simplicity and to provide robustness to the calculations, 30kW are considered.

Capacity requirements

Half of its maximum electrical power was integrated along 60 minutes to obtain the energy needed.

$$E_{elec} = P_{elec} \cdot t = 15kWh$$

FC project

Power requirement

With an output power of 200 kW, electrical components can reach higher efficiencies. The electrical system efficiency considered was 85%.

$$P_{elec} = \frac{P_m}{\eta_{elec}} = 235kW$$

Capacity requirements

The previous procedure is applied:

1. Measure fuel consumption
   The fuel consumption measured was around 120l in a conventional model after the daily operation journey.

2. Estimate the diesel system efficiency
   Taking into account the dominance of low-speed regions (3-4 knots), an average 20% efficiency is used for the calculations.

3. Calculate the mechanical power required
   Every diesel liter contains approximately 10kWh of thermal energy.

   $E_m = \text{fuel consumption(l)} \cdot \text{diesel thermal energy (J/l)} \cdot \eta_{diesel} = 240kWh$

4. Calculate the electrical power required

   As high efficient motors and controllers are used, an average efficiency 80% was considered.

   $E_{elec} = \frac{E_m}{\eta_{elec}} = 300kWh$

3.6 Projects architecture

Hybrid project

From the different configurations presented in section 2.2.3, the parallel one was selected. The energy storage system consists of a lithium-ion battery set. A DC/AC bidirectional converter connects the batteries with the electrical machine and a DC/DC converter connects them with the auxiliary electric loads.

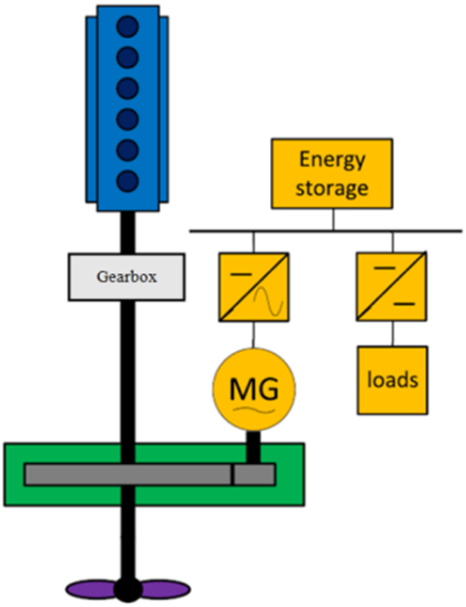

FIGURE 3.5: Architecture hybrid project

Both motors are connected to the shaft through gearboxes with a speed ratio of 2, therefore, the shaft speed is half the motor speed driving the vessel. The engine gears are controlled with two electric valves. Through the pre-charge resistance and switch the voltage rise is limited when the batteries are connected. The extra switch allows disconnecting the batteries from the network (the internal batteries switch is controlled by their battery management system). Low voltage batteries guarantee energy supply even in case of DC/DC failure. Additionally, fuses are used to limit components damage in case of excessively high currents, mainly caused by short-circuits.

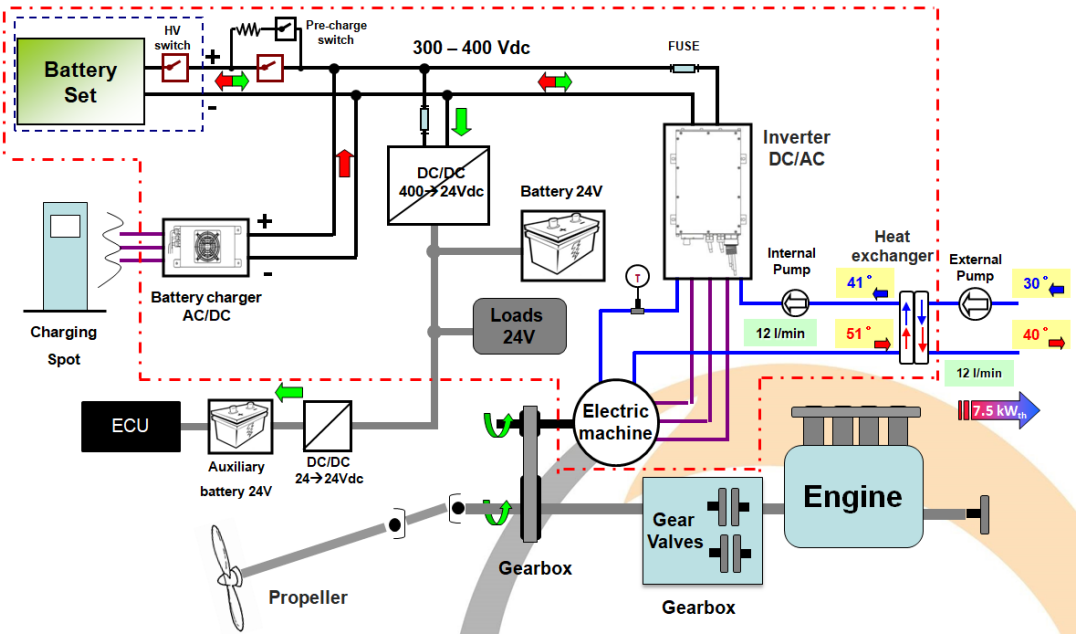

FIGURE 3.6: Detailed scheme hybrid project

The system requirements can be translated into components requirements:

$$P_{bat} = 30kW$$

$$E_{bat} = 15kWh$$

$$P_{mot} = 22kW$$

FC project

In this project, long operation cycles are combined with high power peak demands. While using batteries would significantly limit is operating time, using just a fuel cell of 235 kW would imply huge costs for the project. The energy storage system is again a lithium-ion battery and a fuel cell and a DC/DC converter substitute the diesel engine. This DC/DC converter adapts the fuel cell voltage to the batteries voltage and sets the fuel cell current (the fuel cell acts as a passive component). The rest of the architecture is analog to the previous project, however, the electric machine acts just as a motor and no gearboxes are needed.

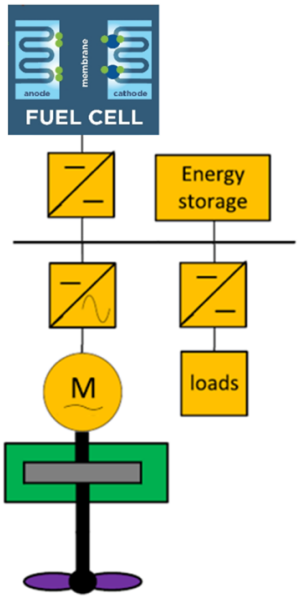

FIGURE 3.7: Architecture FC project

More components are present in this project and two low voltages levels are required, 12 and 24V. A diode ensures that no current is introduced in the fuel cell at low currents. To avoid diode losses, the switch is closed when the fuel cell current is sufficiently high. Due to space limitations, the cooling systems schemes are not included and can be observed in section 6.4.

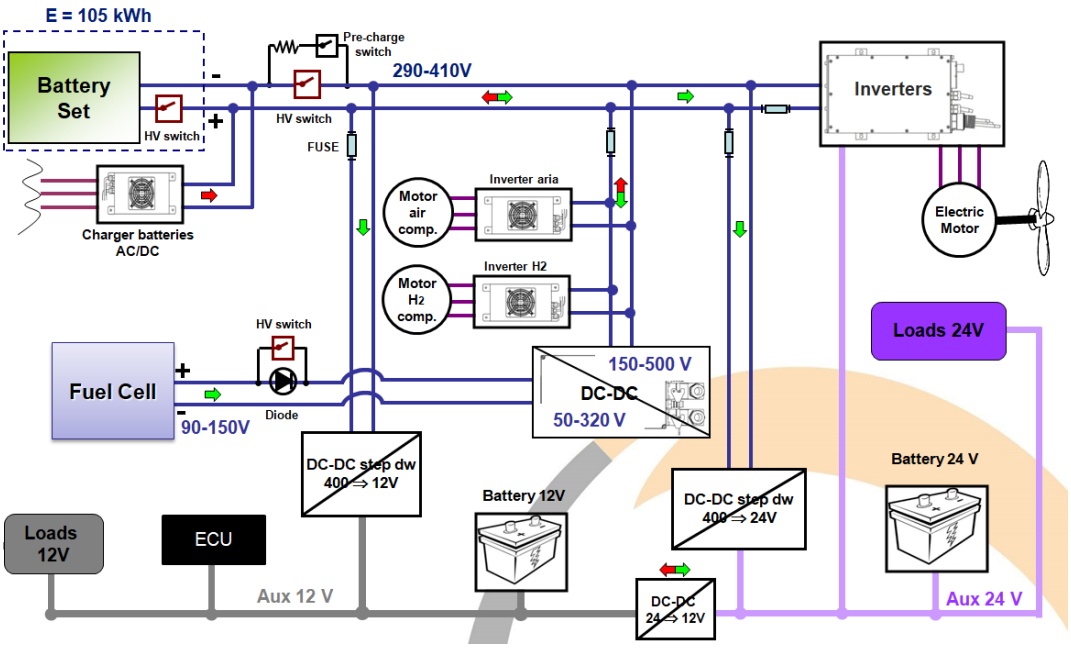

FIGURE 3.8: Detailed scheme FC project

The energy stored in the batteries at night has a significantly lower price per kW compared to the fuel cell produced one. Additionally, increasing the battery capacity provides some extra autonomy to the vessel even if there was no hydrogen. Therefore, the battery capacity was increased as much as possible until a battery weight of 1000kg was achieved (this limit was established to avoid modifying the vessel performance). Finally, according to the autonomy requirements, the fuel cell was selected to provide the rest of the energy.

The battery set selected has a useful capacity of 100 kWh. Considering that the fuel cell can be operating 10h per day, the components requirements are:

$$P_{mot} = 170kW$$

$$P_{bat} = 200kW$$

$$E_{bat} = 100kWh$$

$$P_{fc} = (E_{elec} - E_{bat})/t_{operation} = 20kW$$

$$E_{fc} = P_{fc} \cdot t_{operation} = 200kWh$$

Chapter 4

Power sources

4.1 Diesel engine

The diesel engine and its gearbox were already selected by the client so they're out of the thesis scope and the Dolomitech project. However, they are commanded by the global electronic control unit (it is in charge of turning the engine on/off and commanding its speed and gear). Unfortunately, the diesel engine technical information is limited to the one provided in table 4.1.

TABLE 4.1: Diesel engine characteristics

Maximum speed	2500 rpm
Maximum output power	200 kW
Commands/data flow	BUSCAN Interface

Before connecting a motor to the engine it must have the shaft speed to reduce the mechanical stress. Therefore, the diesel engine must achieve the shaft speed before attaching to it.

4.1.1 Hybrid concept

The concept of specific fuel consumption (SFC) plays a crucial role in understanding the idea of hybrid propulsion. The SFC represents the amount of diesel required to produce one kilowatt-hour (kWh) of energy. A different engine SFC is display to show how it varies according to the speed and power required (figure 4.1). The objective is to keep the engine in a region with a low SFC, or in other words, to keep the engine in its efficient regions.

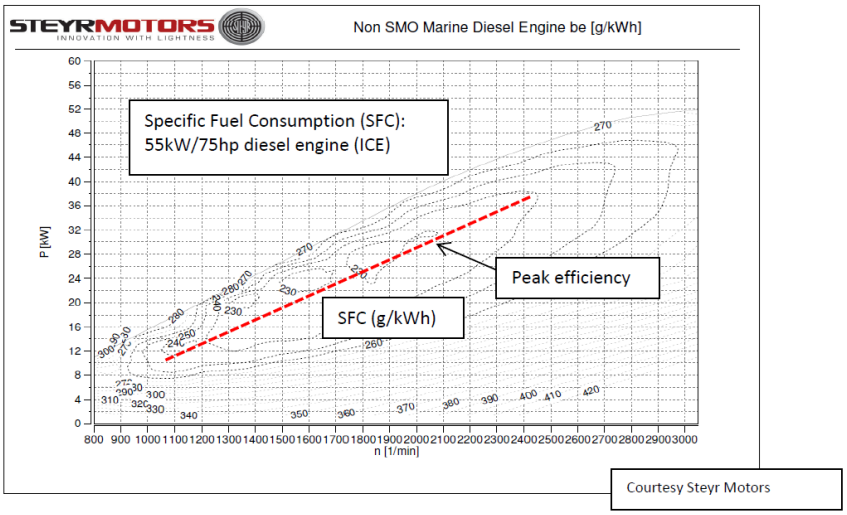

FIGURE 4.1: SFC plot [3]

The engine operation point lays where the engine and propeller power curves match. In figure 4.2 is shown how the propeller power curve and the engine efficient regions do not generally match. The engine and propeller must be selected so that the vessel achieves the maximum speed desired. The exponential shape of a propeller power curve results in low loads at lower speeds, forcing the engine to operate in inefficient regions.

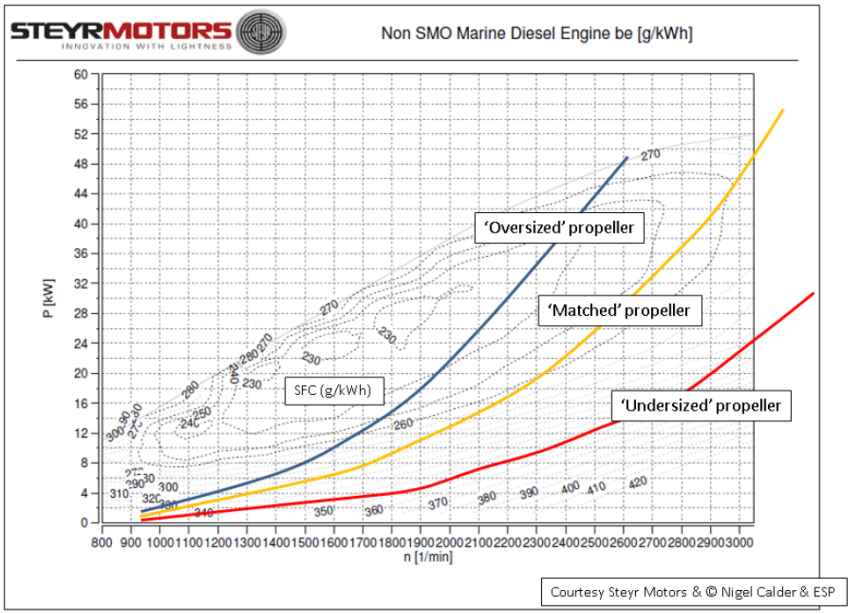

FIGURE 4.2: Propeller power plot [3]

Hybrid powertrains allow turning off the ICE at low speeds, which are the most inefficient regions. The energy is stored at medium or high speeds (efficient regions) using the electric machine as a generator and adding load to the engine. This extra load can be used to increase engine efficiency as it is shown in figure 4.3.

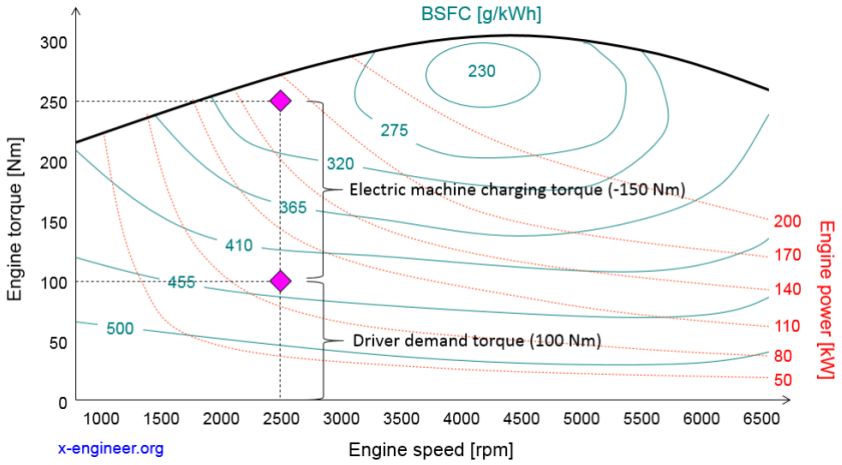

FIGURE 4.3: Electric torque effect on engine performance [11]

4.1.2 Diesel & electric limit

It is necessary to establish an shaft speed limit between the electric and diesel mode. The power requirements can be approximately translated into shaft speed requirements. The propeller power demand is proportional to the angular speed cubed[34].

$$P_{propeller} \propto n^3 \quad \rightarrow \quad \frac{P_1}{P_2} = \frac{n_1^3}{n_2^3} \tag{4.1}$$

In section 3.5, it was established a maximum propeller electric power around 22 kW. Additionally, we know that the power demand at the maximum diesel speed is 170 kW.

$$n_{elec,max} = \sqrt[3]{\frac{P_{n_{elec,max}}}{P_{n_{diesel,max}}}} \cdot n_{diesel,max} \approx 1265\ rpm \tag{4.2}$$

When the sea tests were performed, this limit was slightly reduced to 1150 rpm. Therefore, the engine starts working when a speed higher than 1150 rpm is demanded.

4.1.3 Electric recharging torque

When the electric machine is acting as a generator, the electrical power charged is regulated controlling the torque applied to the shaft. This toque is proportional to the electric current in the electric machine.

The engine torque overcomes the electric brake torque due to the higher engine output power. If the electric speed command is significantly lower than the diesel one, the electric machine can not reach it and it breaks the shaft with the current limit commanded. Adopting this method, the mechanical torque applied is controlled using the maximum current command sent to the inverted. The relation between the torque and current can be considered linear and the constant that relates them can be obtained from the nominal values (section 5.2.2).

$$\tau = k \cdot i \quad \rightarrow \quad k = \frac{\tau}{i} = \frac{\tau_{nom}}{i_{nom}} \approx 1.45\ Nm/A \tag{4.3}$$

The mechanical charging power is obtained by multiplying the torque by the shaft speed.

$$P_m = \tau \cdot \omega = k \cdot i \cdot \omega \tag{4.4}$$

The control is limited by the the electric machine selected can work with a maximum continuous current of 135 arms. Additionally, the maximum electrical charging power of the batteries is 34,1kW in the worst conditions (with a 0% SoC)(section 5.1.4).

The charging current is initially high to counterbalance for the low speeds and increase the power. At high speeds, the charging power is decreased to avoid modifying excessively the vessel performance (figure 4.4). The maximum charging current is 130 arms, which equals to a torque of 189 Nm, and the maximum mechanical charging power is 35 kW. This power does not exceed the battery limits after applying the conversion efficiency, which is lower than 90%.

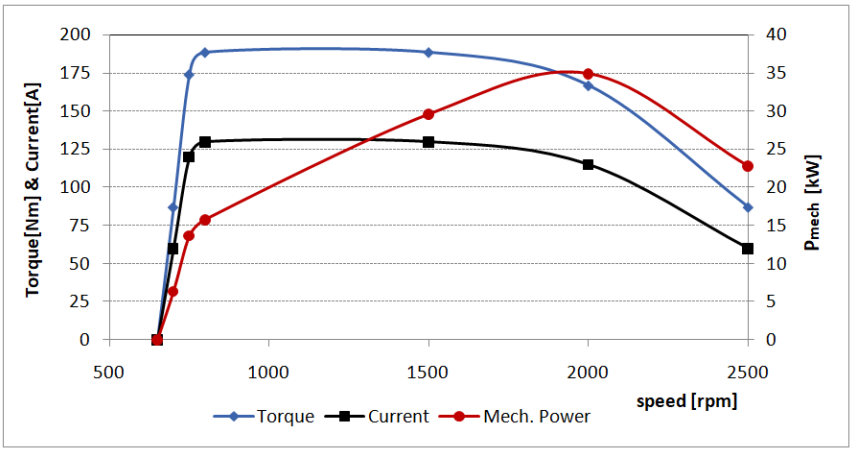

FIGURE 4.4: Charging parameters

The diesel engine is not considered turned on until a speed of 650 rpm is achieved, so bellow this speed no charging torque is applied. To avoid an abrupt load increase that could turn off the engine, the current is initially incremented with a ramp.

At maximum speed the charging mechanical power is 22.7 kW, reducing the maximum vessel power to a value around 150 kW. This power reduction implies a 4% reduction of the maximum angular speed. During the sea test the client was satisfied with the maximum output power still remaining.

$$n_{max} = \sqrt[3]{\frac{P_{max}}{P^0_{max}}} \cdot n^0_{max} \approx 2390\ rpm$$

4.2 Fuel cell

The fuel cells are static devices based on electrochemical reactions that convert chemical energy into electrical energy (oxygen and hydrogen are combined to produce electricity and water). Whereas batteries need to be recharged to provide electricity, fuel cells can produce electricity as long as the fuel is fed. Compared to the internal combustion engines, which produce mechanical energy, the fuel cells generate electricity directly.

The main elements of a fuel cell are the anode, cathode, and electrolyte. The fuel is fed to the anode (positive terminal) and the oxidant is fed to the cathode (negative terminal) and both catalyze the chemical reactions. Pure Hydrogen or gases that contain it (methanol) can be used as fuel, whereas pure oxygen or gases that contain it (air) can be used as oxidant.

$$H_2 \rightarrow 2H^+ + 2e^- \text{ (Anode)} \tag{4.5}$$

$$O_2 + 4H^+ + 4e^- \rightarrow 2H_2O \text{ (Cathode)} \tag{4.6}$$

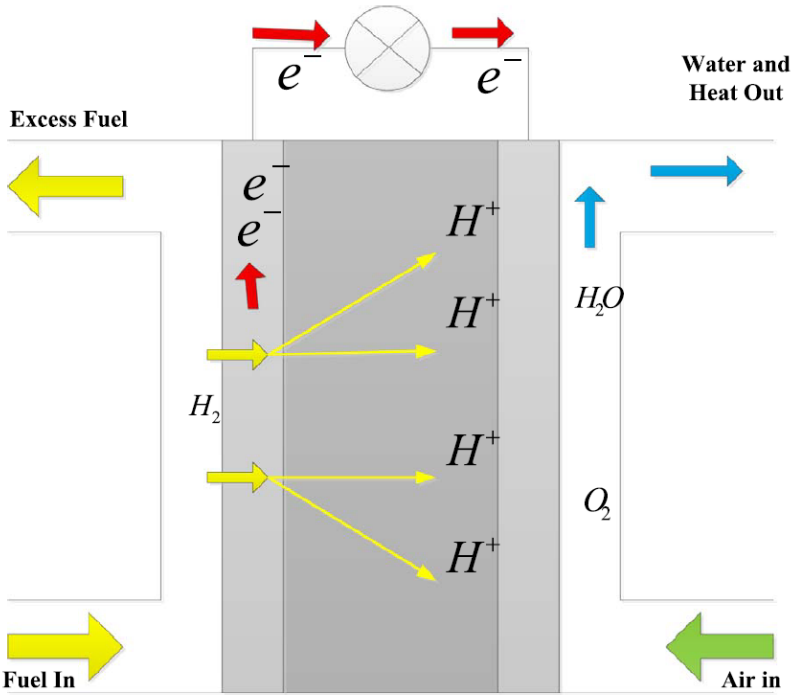

FIGURE 4.5: Fuel cell performance [12]

Hydrogen is decomposed into their ion form in the anode according to equation 4.5. The ions, attracted by the oxygen, pass through the electrolyte located between the anode and the cathode. The electrons cannot pass through the electrolyte and are forced to pass through an external circuit, providing electricity to the load. In the cathode, hydrogen and oxygen are recombined to produce water (equation 4.6).

4.2.1 State of the the art

The fuel cells are classified into different groups, from which the most developed ones are:

- Proton exchange membrane fuel cell (PEMFC)
- Alkaline fuel cell (AFC)
- Phosphoric acid fuel cell (PAFC)
- Molten carbonate fuel cell (MCFC)
- Solid oxide fuel cell (SOFC)
- Direct methanol fuel cell (DMFC)

A comparison between the different technologies is shown in table 4.2. The thesis focuses on PEMFC as it is the most popular one in the transportation sector and the one used in the project.

TABLE 4.2: Fuel cell types [30]

Fuel cell type	Fuel	Cell voltage	Operating temperature (°C)	System output (kW)	Electrical efficiency (%)	Applications
AFC	Pure H2	1.0	90–100	10–100	60	Military, Space
PAFC	Pure H2	1.1	150–200	50–1000	>40	Distributed generation
SOFC	H2, CO, CH4, other	0.8–1.0	600–1000	<1–3000	35–43	Auxiliary power, Electric utility, Large distributed generation
MCFC	H2, CO, CH4, other	0.7–1.0	600–700	<1–1000	45–47	Electric utility, Large distributed generation
PEMFC	Pure H2	1.1	50–100	<1–250	53–58	Backup power, Portable power, Small distributed generation, Transportation
DMFC	CH_3OH	0.2–0.4	60–200	0.001–100	40	mobiles, computers and other portable devices power

Proton exchange membrane fuel cell (PEMFC)

The transportation sector is characterized by strict space constrains and quick start and shut down requirements [35]. Proton exchange membrane fuel cells dominate the sector due to their high power and current densities, compactness, reduced weight, fast output power adjustment and low-temperature operating point. Another important advantage is their carbon dioxide tolerance. AFC fuel cells, the other main quick start fuel cell, are really sensitive to carbon dioxide that may be present in the air.

The core of a PEMFC cell is the Membrane Electrode Assembly (MEA). It is formed by the proton-conducting electrolyte, cathode/anode porous electrodes, anodic/cathodic catalyst layers, and gas diffusion layers (figure 4.6). The gas diffusion layers provide an electronic connection between the bipolar plates and the electrodes, enhance reactants diffusion and water and heat removal.

Each MEA is inserted between current collector plates or bipolar plates. These plates are in contact with the gas diffusion layers and are cut by the flow channels. They transport the electrons, distribute the fuel an oxidant and enhance water and heat management.

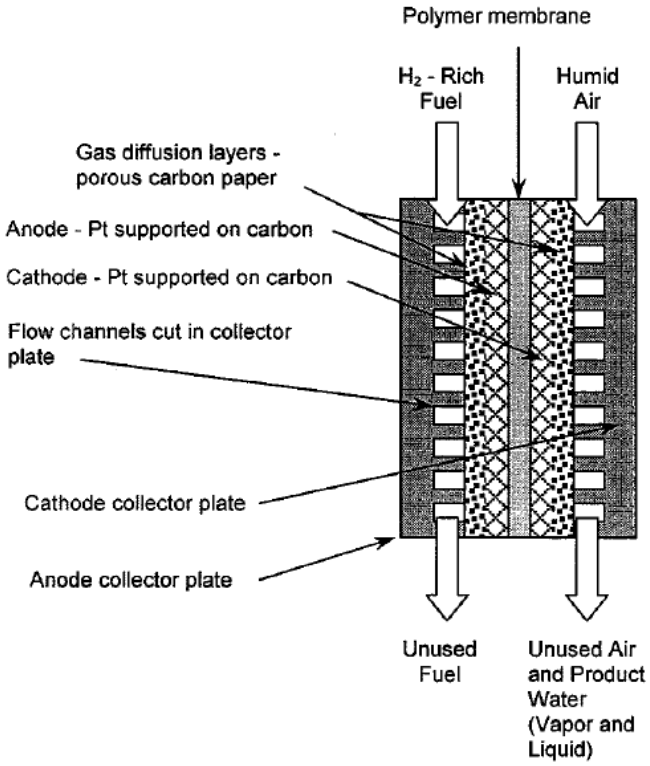

FIGURE 4.6: PEMFC cell structure [13]

Different cells are connected in series to provide a higher voltage (figure 4.7). Coolant plates responsible of the thermal management are placed between cells. In case more current is required different stacks can be connected in parallel.

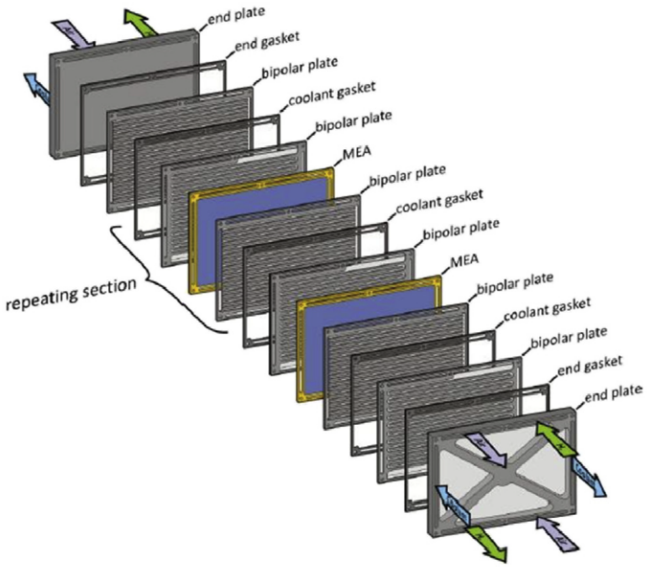

FIGURE 4.7: PEMFC stack [14]

In terms of materials, the electrolyte is made of a Nafion membrane in low-temperature PEM fuel cells (80°C) and a H_3PO_4-PBI membranes in high temperatures PEM fuel cells (110-180°C). As electrodes and electro-catalyst materials, platinum and platinum alloys still dominate the market despite their high price. For the gas diffusion layer, the wet proofed porous carbon cloth or carbon paper with a PTFE(Teflon) coating is preferred. Finally, the bipolar plates are generally made of graphite-based composite materials due to their low density, optimal chemical resistance, and high thermal and electrical conductivity. Nonetheless, depending on the mechanical requirements, metals are also used [14].

Challenges

Achieving acceptable cost and durability performances are probably the main goals os this technology nowadays.

- Fuel cell cost:

  Carbon Trust estimated the necessary cost achievement of \$36/kW to become competitive in the market. Even if mass production can decrease capital, design and fabrication costs, material and components costs must also be reduced

through technological innovation. Platinum is a scarce material and reducing its cost would significantly reduce the fuel cell cost. Using platinum alloys or core shells (nanoscopic metal core covered by a platinum shell) with affordable metals, such as Copper (Cu) or Rhenium(Rh), could be a solution [14]. Besides, platinum could be replaced with other active metals such as Cobalt(Co) or Iron(Fe).

Research efforts are leading to innovative solutions such us the ACAL Energy's patented FlowCath. It uses a liquid polymer cathode that could increase the durability and reduces the platinum required by more than 65%. It had a projected fuel cell cost of 36 $/kW [14]. Another remarkable patent is the one developed by ITM Power's which substituted the conventional perfluorosulfonic acid membranes with ionic polymers membranes. It achieved higher power densities and smaller and lighter stacks with a projected cost of 35 $/kW.

- Durability and performances

  The main causes of degradation are related to insufficient water managements, fuel or oxidant starvation, corrosion and chemical reactions which cause dehydration or flooding [14]. While dehydration damages the membrane, flooding causes corrosion in the different MEA components. Optimal control of flow conditions and new materials will be necessary to increase fuel cells durability.

  In 2017 US Department of Energy (DoE) established the fuel cell durability objective in vehicles in 5000h with a maximum degradation of 10%. Projects like the one presented by ACAL Energy Ltd in 2013 show the potential of fuel cells. PEM hydrogen fuel cells, which use a liquid acting as a catalyst and cooler instead of a platinum catalyst, achieved durabilities of 10.000h.

Finally, hydrogen infrastructure and improvements in hydrogen storage will be necessary. The lack of an extended hydrogen infrastructure significantly affects the sales and hydrogen storage systems are still too heavy and expensive. In addition, hydrogen is mainly produced from natural gas reformation, causing contamination. In the future, hydrogen should be produced from renewable sources such as solar energy or biomass.

4.2.2 Thermodynamics

The Gibbs free energy of a reaction represents the maximum amount of energy per mole that could be converted in work if the volume and the pressure remained constant. A negative Gibbs free energy value indicates that energy is released. Gibbs free energy can be calculated using the following equation:

$$\Delta G_f = \Delta H_f - T\Delta S_f \tag{4.7}$$

ΔH_f and ΔS_f are the enthalpy and entropy differences of formation between the products and the reactants. ΔH_f measures the energy liberated or absorbed by a reaction whileΔS_f indicates the change of molecular disorder. Finally, T represents the temperature of the reaction in Kelvin.

In our case, the hydrogen and oxygen react to form a liquid or water vapor. The Gibbs free energy varies depending on the water state and its values at 25ºC [31]:

$$\Delta G_{H_2O_{(g)}} = -228,57kJ/mol \qquad \Delta G_{H_2O_{(l)}} = -237,13kJ/mol$$

In heat engines, the maximum heat percentage that can be transformed into useful work is limited by the Carnot efficiency (equation 4.8). Ti and Te are the input and output temperatures respectively. To obtain a maximum ideal efficient in fuel cells, reversible efficiency is used. ΔH_f is considered the energy input to our system and ΔG_f defines the maximum amount of energy which can be transformed into work.

$$\eta_{Carnot} = \frac{T_i - T_e}{T_i} \qquad \eta_{rev} = \frac{\Delta G_f}{\Delta H_f} \tag{4.8}$$

The electrical work per mole can be obtained using the equation 4.9. F represents the Faraday's constant (96,485 C/mol), E the potential or voltage and n the number of electrons per molecule of H_2, which is 2 [15].

$$W_{elec} = nFE \tag{4.9}$$

Supposing ideal conditions, all the free Gibbs energy would be transformed into electrical work. Under these conditions, the voltage obtained is known as reversible or Nernst voltage. Two different values are obtained depending on the water final state (a temperature of 50°C is considered to calculate the values).

$$E_{rev} = -\frac{\Delta G_f}{nF} \tag{4.10}$$

$$E_{rev,\,g} = -\frac{\Delta_f G_{H_2O(g)}}{2F} = 1.178V \qquad E_{rev,\,l} = -\frac{\Delta_f G_{H_2O(l)}}{2F} = 1.208V$$

The temperature has a significant influence on the Gibbs free energy. When the temperatures increases, Gf decreases in magnitude.

TABLE 4.3: Free energy of Gibbs vs temperature [31]

T [°C]	-25	0	25	50	100	200	400	600	800	1000
$\Delta G\ H_2O_{(g)}$ [kJ/mol]	230.8	229.7	228.6	227.5	225.2	220.4	210.3	199.7	188.7	177.5
$\Delta G\ H_2O_{(l)}$ [kJ/mol]	245.4	241.3	237.1	233.1	225.2	210.0	199.0	230.4	267.1	308.3

Consequently, the available maximum work, the reversible efficiency and the Nernst voltage decrease with temperature. However, real voltages and efficiencies increase at higher temperatures due to the reduction of losses (section 4.2.3).

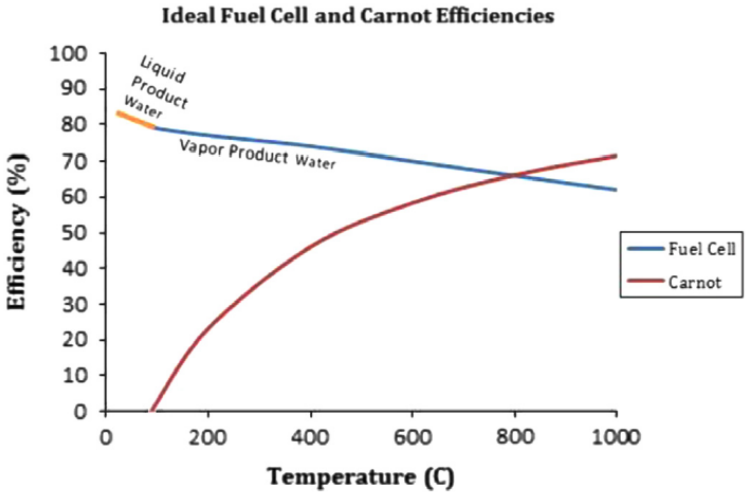

FIGURE 4.8: Ideal fuel cell efficiency (using $\Delta H_{H_2O_{(l)}}$) vs carnot efficiency (with an exhaust temperature of 90°) [15]

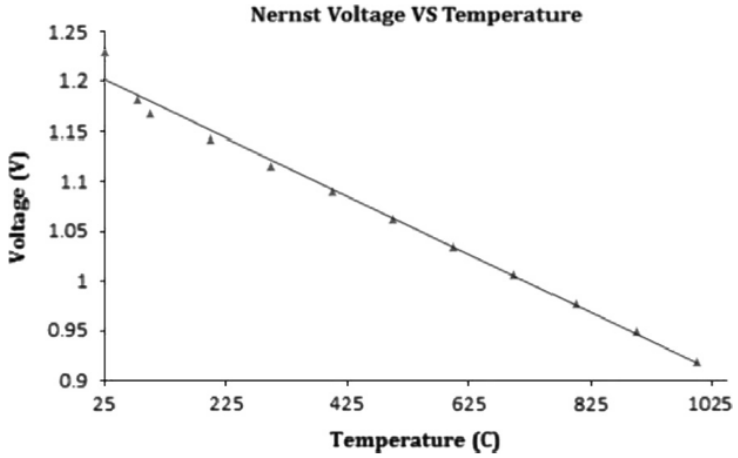

FIGURE 4.9: Nernst voltage with respect to temperature in a hydrogen/oxygen PEMFC at 1 atm [15]

Pressure also plays an important role in Gibbs free energy. The relation is shown in Equation 4.11, where the zero superscript references the values to standard conditions (1atm and 25°C), R represents the gas constant and the different P's represents the gases partial pressures.

$$\Delta G_f = \Delta G_f^0 - RT \ln\left(\frac{P_{H_2} P_{O_2}^{0.5}}{P_{H_2O}}\right) \tag{4.11}$$

Applied to the Nernst Voltage, the following equation is obtained:

$$E_{rev} = E_{rev}^0 + \mathfrak{R}\mathfrak{T} nF \ln\left(\frac{P_{H_2} P_{O_2}^{0.5}}{P_{H_2O}}\right) \tag{4.12}$$

Consequently, decreasing reactants pressures or concentrations results in Nernst voltage reductions. For example, the Nernst voltage drop when using air instead of pure oxygen is equal to:

$$\Delta E_{rev} = \frac{RT}{2nF} \ln\left(\frac{1}{0.21}\right)$$

4.2.3 Polarization curve

In real operation, numerous losses lead to significant differences between the real and Nernst voltage. They can be categorized in crossover, activation, ohmic and concentration losses. All of them are present in the entire polarization curve (V-I performance of the fuel cell), however, each of them dominates different segments (figure 4.10). The thermoneutral voltage concept is explained later in section 4.2.5.

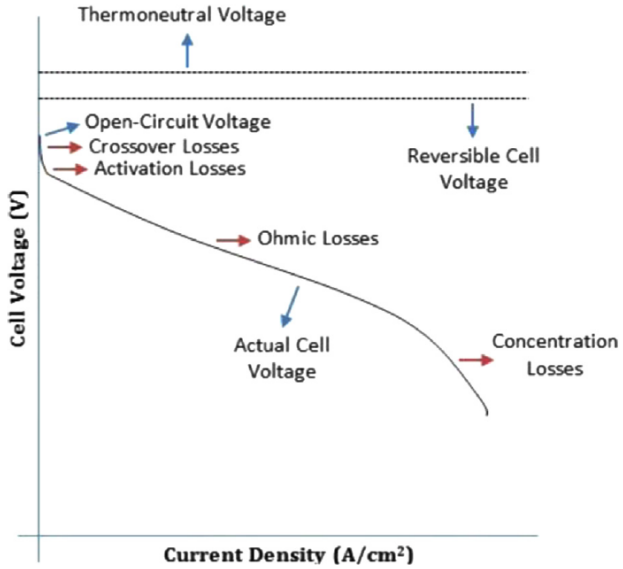

FIGURE 4.10: Polarization curve [15]

Crossover losses

They dominate the open circuit losses. Even if the electrolyte membrane is almost impermeable, some direct hydrogen fuel diffusion without anodic reaction occurs. Additionally, some electrons cross the membrane instead of the external circuit. When the current density increases, the hydrogen gradient through the membrane decreases and so does the diffusion force. Increasing the operating temperature or membrane's permeability or thickness reduces these losses.

Activation losses

They are dominant at low current densities. Cathode and anode reactions need the energy to start, so slow oxidation and/or reduction kinetics lead to a voltage drop. These losses are present in both electrodes, however, the reduction losses dominate in hydrogen fuel cells. These losses can be reduced by increasing electrode activity, especially on the cathode side. Choosing an active electrode catalyst or increasing the operation temperature, surface roughness, catalyst loading or reactants concentration and pressure (optimizes the actives spots on the electrode area) are some of the main solutions to decrease these losses [15]. Catalyst contaminants and long operating cycles should also be avoided. Even if the ideal voltage is reduced with temperature,

the activation losses reduction decrease faster and the real voltage is increased with temperature.

Ohmic losses

They are especially important at intermediate current densities and are caused by the electric and ionic resistance of the different stack components. While the conductive components of the electronic flow have an electrical resistivity and the electrolytic membrane has it against the ionic flow. Both together, explain the ohmic voltage drop, however, the ionic one dominates in general. The ionic conductor's capacity to carry charge is significantly lower compared to the electronic conductor's one. Using materials with high conductivity, minimum thickness and contact resistance can reduce these losses.

Concentration losses

They dominate the high current density segment of the curve. They occur when electrode reactions are limited due to the lack of reactants. It can be caused by many reasons such as limited reactants supply or diffusion rates from flow field channels to the catalyst layer, poor air circulation at the cathode which leads to the accumulation of nitrogen (or other inert gases), water accumulation and flooding at the cathode and anode (especially for PEMFCs) or impurities adsorption on electrode reaction areas[15]. These losses grow incredibly faster at high currents reducing the voltage to zero at the end. In figure 4.11 is shown how do each of the losses increase with temperature in a PEMFC example fuel cell (crossover losses are included within activation losses).

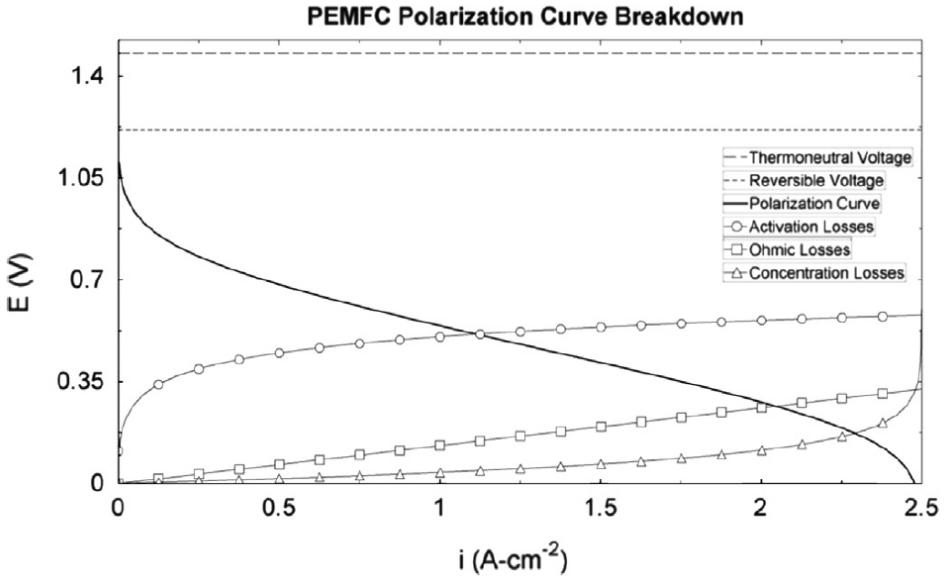

FIGURE 4.11: PEMFC losses [15]

4.2.4 Fuel cell selection

The most recent cell model from the supplier was used in the project. A stack made of 150 cells connected in series was selected. With the following polarization curve (figure 4.12), it can produce up to 38kW. The power margin will be used to deal with battery degradation and reduce fuel cell stress.

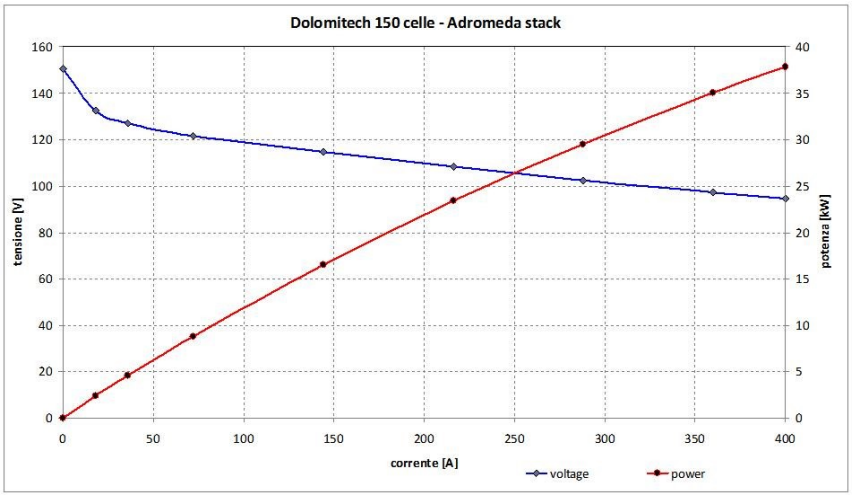

FIGURE 4.12: Stack polarization curve

Instead of a traditional close flow field, the cells have an open flow field. In a close field, the bipolar plate is directly connected to the gas diffusion layer, while in the open field both are connected through a metallic foam (figure 4.13).

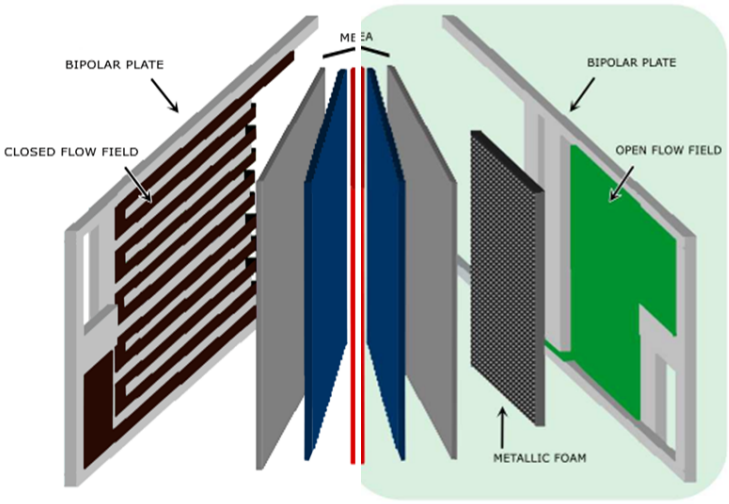

FIGURE 4.13: Close field vs Open field

This structural modification improves its performance, however, it has disadvantages at low currents. Its performance impact consists of:

- Reactants diffusion improvement at high currents
- Ohmic resistance reduction.
- Worse reactants diffusion and more water management issues at low currents.

The fuel cell also includes a cell voltage monitor (CVM). It continuously measures and transmits each cell voltage in order to detect possible problems.

4.2.5 Heat Management

Operating temperature

If the temperature increases, activation losses decrease faster in magnitude than the Gibbs free energy. Consequently, the fuel cell real voltage increases (figure 4.14). Nevertheless, increasing the temperature also implies the increase of the thermal stress on the fuel cell.

An operation temperature of 50°C was considered the optimal equilibrium between performance and durability. The fuel cell temperature is increased with its own heat produced and the cooling system keeps it in the desired value. The fuel cell cooling system is discussed in section 6.4.2.

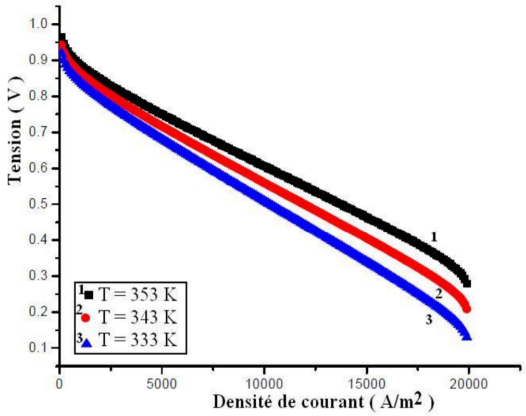

FIGURE 4.14: Temperature effect on PEMFC polarization curves [16]

Heat calculation

The thermal energy produced in a fuel cell can be estimated using the energy balance represented in figure 4.15. The input energy to the system must be equal to the output energy, or in other words, the enthalpy difference between products and reactants must be equal to the sum of the electrical energy and the heat generated.

$$\sum(h_i)_{in} = W_{elec} + \sum(h_i)_{out} + Q$$

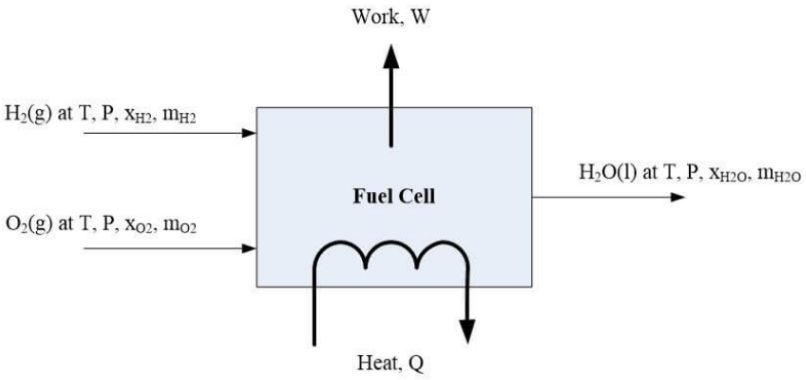

FIGURE 4.15: Fuel cell energy balance [17]

The enthalpy of liquid water formation is known as higher heating value (HHV) and the enthalpy of vapor water formation is known as lower heating value (LHV). Both values differ in the latent heat of water vaporization. Their values depending on the temperature are shown in table 4.4.

TABLE 4.4: Heating values vs temperature

T [°C]	-25	0	25	50	100	200	400	600	800	1000
LHV [kJ/mol]	241.3	241.6	241.8	242.1	242.6	243.5	245.3	246.9	248.2	249.3
HHV [kJ/mol]	287.4	286.6	285.8	285.0	283.4	280.0	265.8	242.3	218.8	195.3

To simplify the equations it is considered that all the thermal energy is transformed into electricity, obtaining the so-called thermoneutral voltage. It cannot be achieved in reality, even in the ideal case, part of the energy must be used in the entropy change. It has two different values according to the heating value used.

$$E_{LHV_{50^oC}} = \frac{LHV_{50^oC}}{2F} = 1.255V \qquad E_{HHV_{50^oC}} = \frac{HHV_{50^oC}}{2F} = 1.477V \tag{4.13}$$

Finally, to obtain the heat produced related to the fuel cell current, real measurements are used. According to the energy balance 4.15, the heat produced is equal to the enthalpy of water formation minus the electrical work. This implies that the heat produced is equal to the difference between the thermoneutral and real voltage multiplied by the current.

$$Q = (E_{thermoneutral} - E_{real})i \tag{4.14}$$

During the fuel cell operation, both liquid and vapor water are produced. In the tests performed at 55°C, it was observed that the vapor was dominant. Therefore, a thermoneutral voltage of 1.3V is used for the calculations. Using the polarization curve (figure 4.12) to obtain the real electric values, the estimated heat produced is:

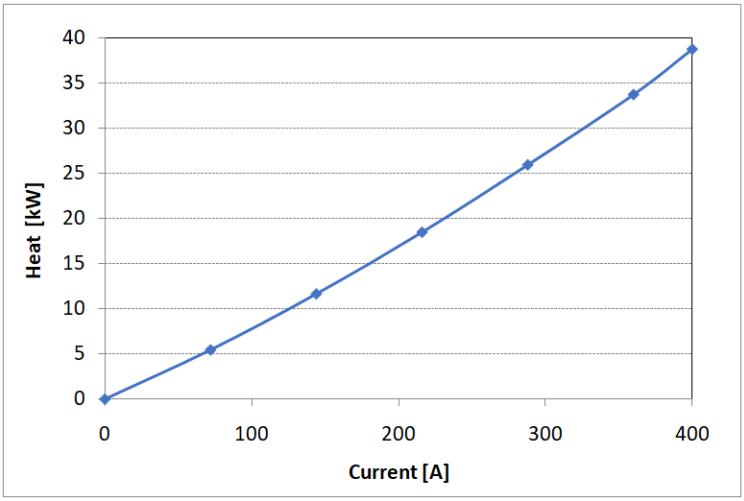

FIGURE 4.16: Heat generation of the fuel cell

4.2.6 Flow rates

Hydrogen and oxygen fluxes depend on the fuel cell current. Applying Faraday's law the follow, the equation 4.15 is obtained.I is the fuel cell current in A, $\dot{n}$ the mole flow in mole per second, z the number of electrons in the reaction and F the Faraday constant:

$$I = \dot{n}zF \tag{4.15}$$

Considering our reactions; (equations 4.5 & 4.6) the hydrogen, oxygen and water fluxes are:

$$\dot{n}_{hydrogen} = \dot{n}_{water} = \frac{I}{2F} \qquad \dot{n}_{oxygen} = \frac{I}{4F} \tag{4.16}$$

The relation between the reactants supplied and consumed is established by the stoichiometric ratio λ.

$$\lambda = \frac{\dot{n}_{feed}}{\dot{n}_{consumed}} \tag{4.17}$$

Molar weights, stoichiometric ratios and the number of cells are added to the previous equations to express the total flows in grams per second. If air is used as oxidant, the oxygen fraction in the air must be also added to the equation.

$$\dot{m}_{hydrogen} = \lambda \frac{I \cdot 2.016 \cdot num_{cell}}{2F} \tag{4.18}$$

$$\dot{m}_{oxygen} = \lambda \frac{I \cdot 31.988 \cdot num_{cell}}{4F} \tag{4.19}$$

$$\dot{m}_{air} = \lambda \frac{I \cdot 31.988 \cdot num_{cell} \cdot 4.32}{4F} \tag{4.20}$$

$$\dot{m}_{water} = \frac{I \cdot 18.01 \cdot num_{cell}}{2F} \tag{4.21}$$

4.2.7 Cathode side

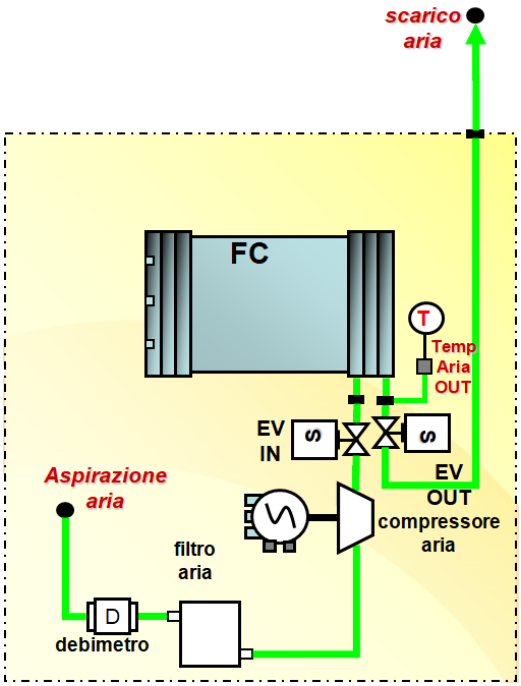

FIGURE 4.17: Cathode side

Oxidant flow

Instead of pure oxygen, air flow is used as oxidant in the fuel cell. The air flow is guaranteed by a compressor that introduces atmosphere air in the fuel cell. To guarantee its supply, the stoichiometric ratio is set around 1.75 (it slightly increases with the current to avoid concentration losses). At low currents, the ratio is higher as a minimum flow must be maintained in the compressor.

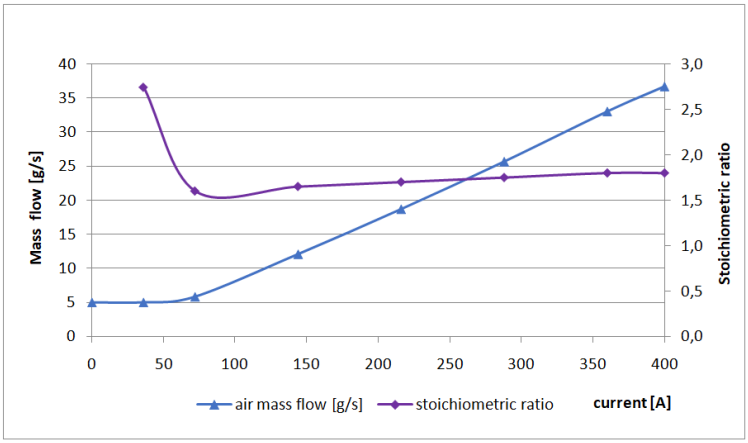

FIGURE 4.18: Cathode air flow & stoichiometric ratio

Cathode pressure

The cathode is provided with valves to increase cathode pressure. Higher oxygen pressures lead to a better fuel cell performance, however, they increase the compressor consumption and fuel cell mechanical stress. Considering the overall system, the valves remain completely open during fuel cell operation.

With the valve completely open, the cathode input pressure is equal to the cathode circuit pressure losses. Higher flows imply higher losses, therefore, higher currents imply higher cathode pressures. Figure 4.19 was obtained from experimental data.

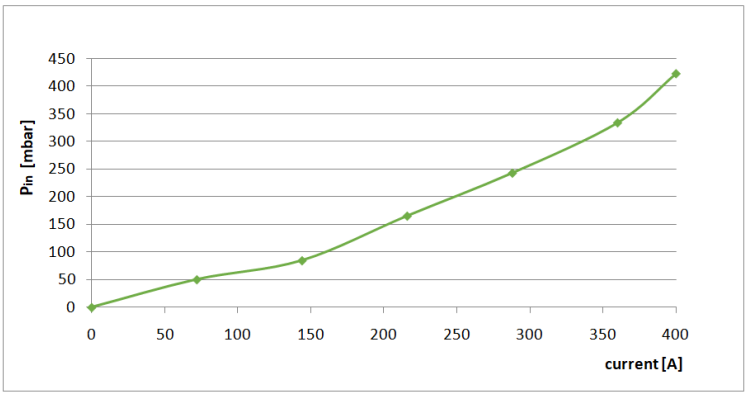

FIGURE 4.19: Input cathode pressure

Compressor

As noise reduction is one of the main attractions of electric vessels, a silent compressor must be used. Besides, it is highly recommended the use of water as a coolant instead of oil. Otherwise, a component failure could end with oil in the fuel cell.

Centrifugal compressors offer better performance characteristics in terms of noise than volumetric compressors. Due to the lack of suitable compressors in the market, Dolomitech developed a centrifugal compressor in previous projects. Its characteristics, obtained from experimental data, are:

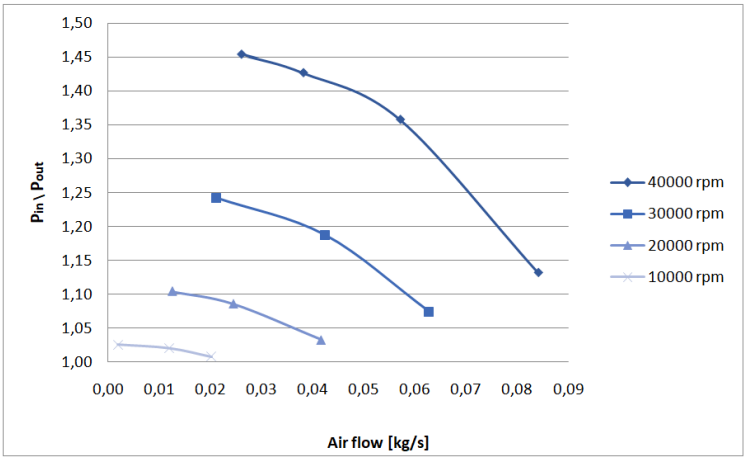

FIGURE 4.20: Compressor pressure ratio vs flow

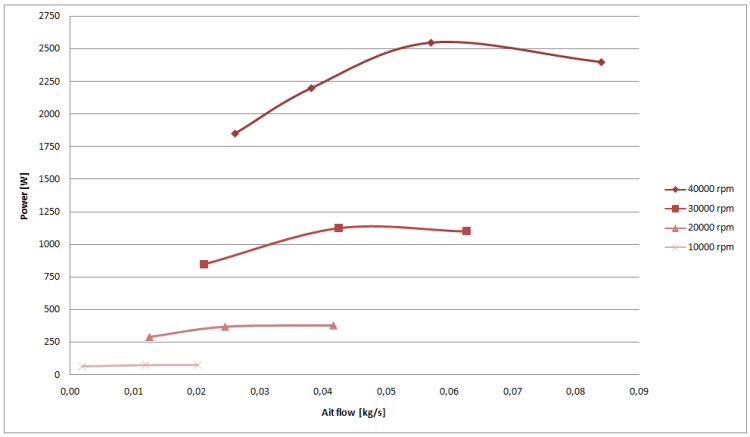

FIGURE 4.21: Compressor power consumption vs flow

The air compressor is the auxiliary component with the highest power consumption of the fuel cell system. The compressor operation point lays where its curve matches the cathode pressure losses. Controlling the compressor speed the demanded flow is achieved. It is controlled by close-loop based on the measured air flux.

4.2.8 Anode side

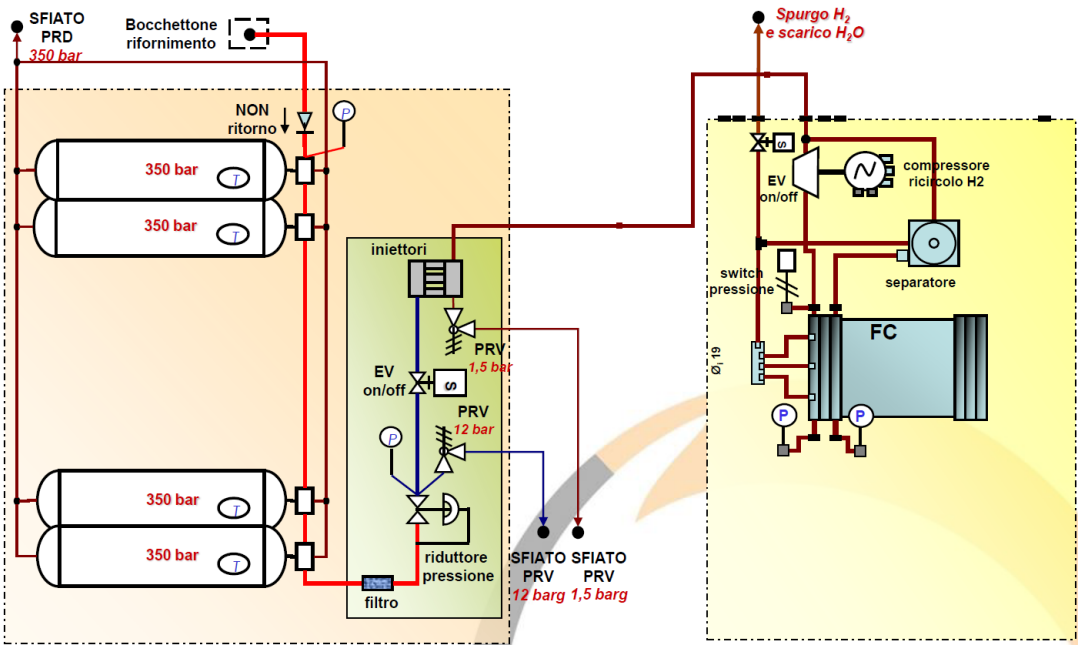

FIGURE 4.22: Anode side

Fuel supply

On the anode side, hydrogen flows in a closed circuit in which a certain pressure is maintained. Higher hydrogen pressures improve fuel cell performance but increase its mechanical stress. According to the supplier information, pressure should not exceed 1.2 bar so, considering that the cathode operates with low pressures, the selected anode pressure is 0.8 bar. For security reasons, some valves were added to ensure that pressure remains under certain values

A set of valves decreases the hydrogen pressure from the tanks before reaching the fuel cell. Initially, just mechanical valves were used but they suffered from durability issues. The mechanical stress was damaging them before the time expected. As a solution, a mechanical valve was used to decrease the pressure to 20 bar and an electrical one to 0.8bar. This last one consists of injectors electrically commanded by the ECU. The ECU receives the measured pressure from a sensor and opens the injectors when it is lower to the desired one.

A compressor, set with a fixed speed, recirculates the hydrogen ensuring its supply. It must be a compact device to void losing hydrogen while operating. In comparison with the cathode side, the circuit pressure drop (below 70mbar) and the volumetric flow are significantly smaller.

Fuel consumption

Fuel consumption can be calculated using equation 4.18, however, fuel losses must be taken into account. According to the tests performed, fuel losses are around 5% at sufficiently high currents. At lower currents, losses are higher, but the fuel cell will not operate in those conditions.

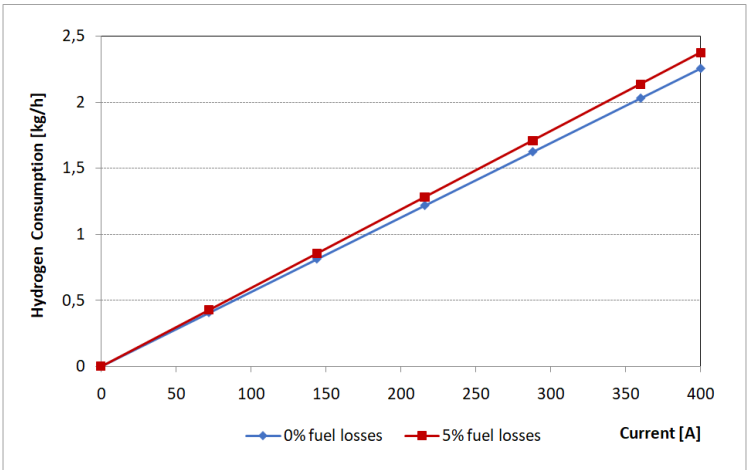

FIGURE 4.23: Fuel consumption

Fuel storage

Fuel is stored in high-pressure tanks, which must be able to store the daily required fuel. Hydrogen is stored in four tanks that stand pressures up to 350 bar. Each of them has an empty weight of 90Kg, an internal volume of 205l and a storage capacity of 5kg. With a total storage capacity of 20kg and considering a 5% of fuel losses, the fuel cell could operate continuously for 10h with currents up to 330A (around 33kW).

TABLE 4.5: Hydrogen storage

Hydrogen capacity	20 kg
Internal volume	820 l
Maximum pressure	350 bar
Total weight charged	380 kg

4.2.9 Water Management

Water management is crucial to prevent cells from flooding or drying out. The goal is to keep the membrane homogeneously hydrated without causing water accumulation. Water is produced continuously in the cathode, where it tends to accumulate. If water accumulates in the electrodes, the gas diffusion layers or the gas channels, reactants can be prevented from reaching catalyst sites. This can cause reactants starvation and increases fuel cell losses. On the other hand, the anode side of the membrane tends to dry out, reducing its protonic conductivity and increasing the cell resistance. This increases the voltage losses and can cause and permanent damages.

When hydrogen moves to the cathode side it carries part of the water with it; this phenomenon is called electroosmotic drag. At the same time, water diffusion occurs due to the gradient between the anode and cathode and water is transferred from the cathode to the anode. Consequently, the total water flow in the cathode is the sum of the water content in the oxidant, the water produced and the difference between the electroosmotic drag and the back-diffusion water. On the anode side, it is equal to the inlet fuel water content minus the difference between the electroosmotic drag and the back-diffusion water.

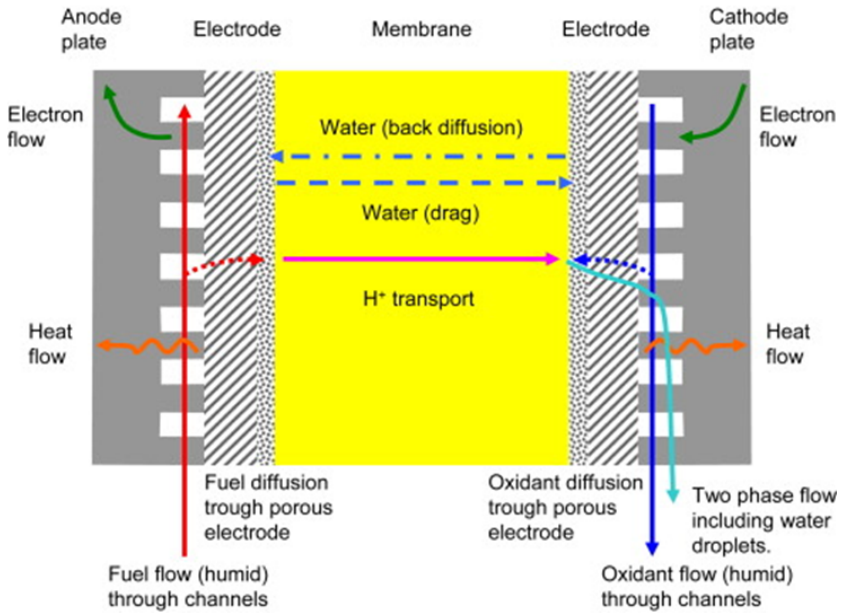

FIGURE 4.24: Water management [18]

Cathode

Unsaturated reactant fluxes remove the water through the flow channels. Low operating temperatures and flow rates reduce the amount of water that reactant gases can remove. Porosity, thickness, and hydrophobicity of the gas diffusion layers and the flow channel geometry are also fundamental factors.

Long cycle tests were performed with currents bellow the expected operating ones(the lower the current, the poorest the water removal capacity). With currents higher than 150 A, the operation temperature and airflow are sufficiently high to properly remove the cathode water. Nonetheless, when turning on and off the fuel cell, the compressor is set to its maximum speed to increase the air flux and dry the fuel cell.

Anode

Depending on the fuel cell current the anode side may dry out or flood. As the inlet hydrogen water content is almost zero, the water generated depends on the difference between the electroosmotic drag and the diffusion effect. To avoid membrane dehydration during high currents, gas humidifier systems are a possible solution. However, they increase weight, size, complexity and parasitic power. Using thinner membranes (higher back diffusion effect), improving the gas diffusion layers or recirculating reactant gases are some other alternatives. In our case, the solutions adopted to avoid dehydration are:

- Hydrogen recirculation
  Hydrogen coming from the tanks has really low water content, nonetheless, after passing through the flow circuit, its water content increases. By recirculating it, the dry hydrogen is mixed with the one already present in the fuel cell with higher water content, preventing the membrane to dry out.

- Limited current demanded
  The fuel cell is expected to operate with 50% -70% of its maximum current (22-30 kW). This limits the electro-osmotic drag effect that dehydrates the membrane.
- Thin cell membrane
- Open field
  Improves gas diffusion and enhances homogeneity at high currents.

In the tests carried out with currents between 200 and 280A, water tended to slightly accumulate in the anode. This was solved by a purge valve periodically activated and connected to:

- Separator
  A separator is located in the hydrogen circuit to get rid of the anode water. The recirculated hydrogen is forced to pass through a hollow cylinder, in which water remains in the walls and falls while hydrogen exits from the upper side.

- Internal fuel cell flow circuit
  The hydrogen circuit inside the fuel cell is provided with some intermediate exits to enhance water removal. They are used, without recirculating them to the separator, to get rid not only of the water but the nitrogen. Otherwise, the small amount of nitrogen able to cross the membrane would accumulate, decreasing continuously hydrogen purity.

4.2.10 DC/DC converter

The fuel cell voltage must be increased before connecting it to the power bus where the batteries and motor are connected. According to the fuel cell and batteries selected, the DC/DC converter operating conditions are:

Table 4.6: DC/DC operating conditions

Maximum input current	400 A
Minimum and maximum output voltage	295-400V
Maximum output power	38kW

The DC/DC converter selected has the following technical characteristics.

Table 4.7: DC/DC technical characteristics

Maximum input current	<500 A
Maximum output voltage	500V
Efficiency	>97 (200V & 400A IN)%
Dimensions	639 x 475 x 158 mm
Weight	35 kg

4.2.11 Efficiencies

Different efficiencies can be defined in a fuel cell, depending on the input and output of the system. The following efficiencies are calculated considering a fuel cell temperature of 50°C. Apparently there is no commitment to name the different efficiencies so different names may be found in other documents.

Reversible efficiency

Equivalent to the Carnot efficiency, it is the maximum ideal efficiency than can be achieved in a fuel cell. It is the ratio between the free Gibbs energy and enthalpy of formation.

$$\eta_{rev} = \frac{\Delta G}{\Delta H} \qquad \eta_{rev\ l} = 81.79\ \% \qquad \eta_{rev\ g} = 93.97\ \%$$

Electric efficiency

Relates the electric power produced with the internal thermal energy contained in the hydrogen consumed. It is obtained by dividing the average cell voltage by the thermoneutral voltage.

$$\eta_{elec} = \frac{P_{elec}}{P_{fuel,consumed}} \tag{4.22}$$

$$\eta_{elec\ l} = \frac{\overline{V}_{cell}}{E_{HHV}} = \frac{\overline{V}_{cell}}{1.477} \qquad \eta_{elec\ g} = \frac{\overline{V}_{cell}}{E_{LHV}} = \frac{\overline{V}_{cell}}{1.255}$$

Fuel electric efficiency

It also considers fuel losses. They were considered a 5% (η_{fuel} is 95%) in section 4.2.8.

$$\eta_{fuel,elec} = \eta_{elec} \cdot \eta_{fuel} \tag{4.23}$$

Voltage efficiency

Ratio between real and reversible voltage.

$$\eta_{voltage} = \frac{\overline{V}_{cell}}{E_{rev}} \tag{4.24}$$

$$\eta_{voltage\ l} = \frac{\overline{V}_{cell}}{E_{rev,l}} = \frac{\overline{V}_{cell}}{1.208} \qquad \eta_{voltage\ g} = \frac{\overline{V}_{cell}}{E_{rev,g}} = \frac{\overline{V}_{cell}}{1.178}$$

The real fuel cell voltage changes with the current demanded, therefore, the efficiencies (except the reversible one) vary with the fuel cell current.

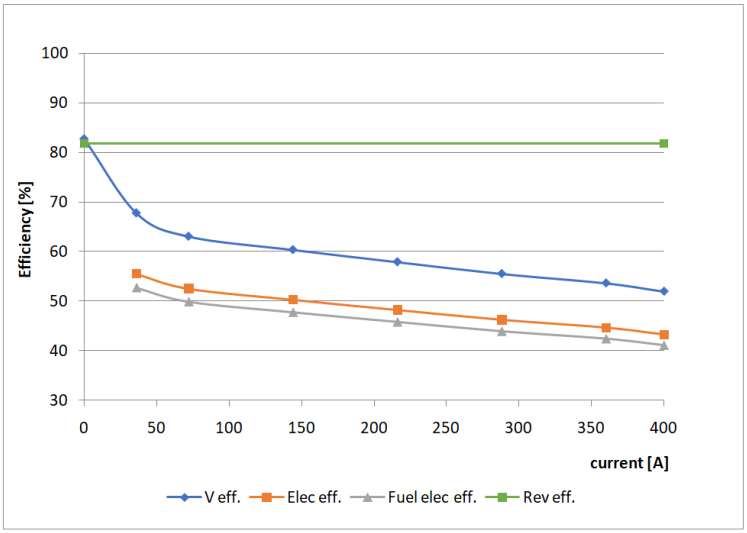

FIGURE 4.25: Fuel cell efficiencies (liquid water)

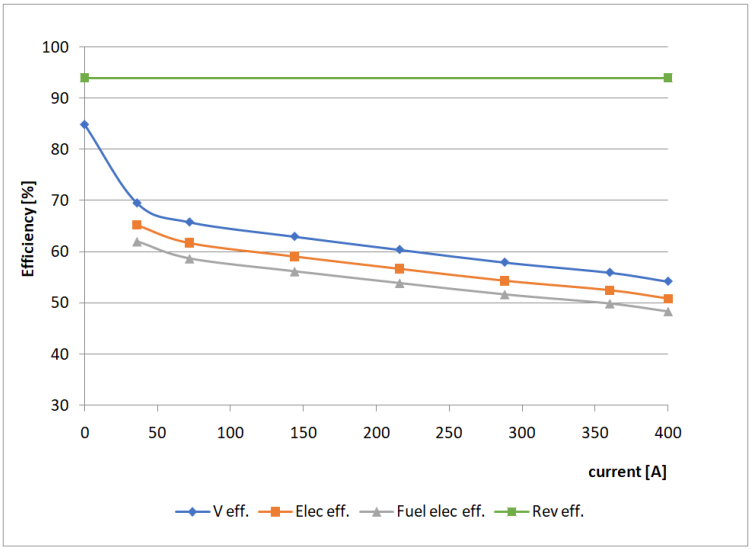

FIGURE 4.26: Fuel cell efficiencies (vapor)

4.2.12 Fuel cell system

In the following scheme, the cooling systems are also included (treated in section 6.4).

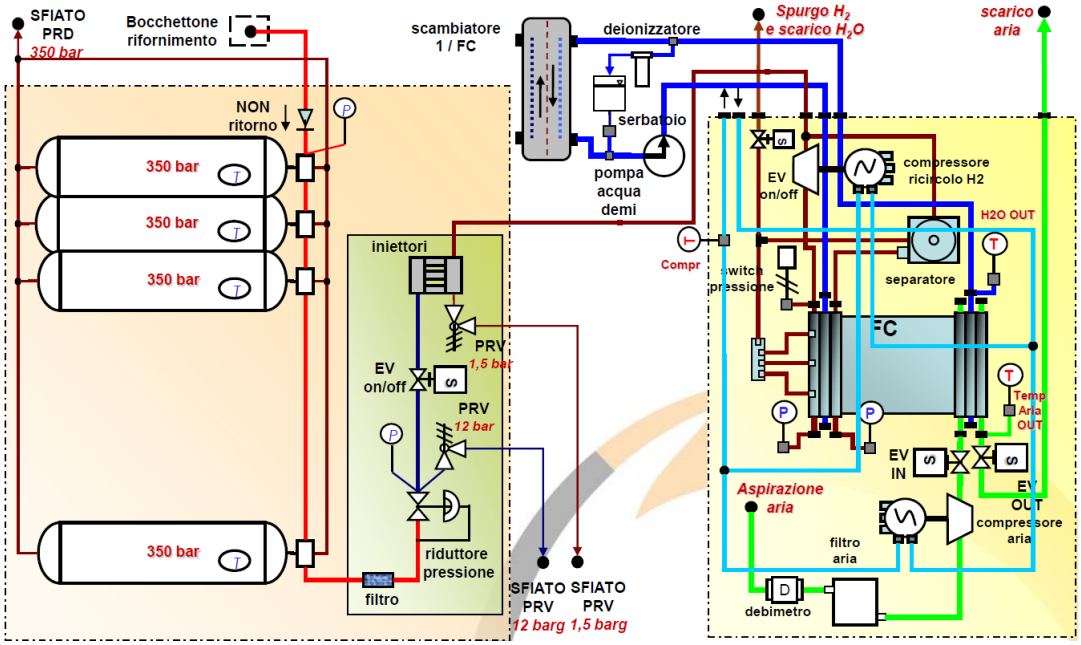

FIGURE 4.27: Fuel cell system scheme

The fuel cell system operates stationary in a fixed operating point. Test during operation will be performed to properly set it, however, it is expected to work with currents between 200 and 280 A (most likely between 200 and 250 A).

TABLE 4.8: Fuel cell system operation points

Current FC [A]	**150**	**200**	**250**	**280**	**350**
Voltage FC [V]	114	110	106	103	98
Power FC [kW]	17	22	26.5	29	34.2
Air flow [g/s]	12.5	17	22	25	32
Cathode P_{in} [mbar]	90	150	200	235	320
Power air comp.[W]*	260	475	700	900	1475
Power hyd. comp.[W]*	300	300	300	300	300

*Power consumption values are approximations from the components curves

To calculate the fuel cell system power, DC/DC efficiency and power consumption of the auxiliary components must be taken into account. The DC/DC efficiency is approximated to 95% and the auxiliary components considered are the air and hydrogen compressors.

$$P_{fcs} = \eta_{dc/dc} \cdot P_{fc} - P_{air\ comp} - P_{H_2\ comp} \tag{4.25}$$

$$P_{fcs\ 150A} \approx 15.6kW \qquad P_{fcs\ 200A} \approx 20.1kW$$
$$P_{fcs\ 250A} \approx 24.2kW \qquad P_{fcs\ 280A} \approx 26.3kW$$
$$P_{fcs\ 350A} \approx 31.3kW$$

Cooling pumps were not considered as their consumption highly depends on the seawater temperature. During the test performed in summer (with an ambient temperature around 30ºC), their total power consumption was around 500W, with currents between 200 and 250 A.

Previous fuel cell efficiencies can be recalculated considering the fuel cell system power as the output power. Efficiencies are just calculated considering liquid water as the product and a fuel cell temperature of 50ºC. Additionally, we can define η_{aux} as the ratio between the fuel cell and the fuel cell system power.

$$\eta_{aux} = \frac{P_{fcs}}{P_{fc}} \quad \rightarrow \quad \eta_x^{fcs} = \eta_x^{fc} \cdot \eta_{aux} \tag{4.26}$$

TABLE 4.9: Fuel cell system efficiencies

FC current [A]	**150**	**200**	**250**	**280**	**350**
FCS aux eff.	91.8	91.4	91.3	91	91.5
FCS voltage eff.	55.1	53.5	51.8	50.7	49.4
FCS elec. eff.	45,9	44.5	43.1	42.3	41.2
FCS fuel-elec. eff.	43.6	42.3	40.9	40.2	39.1

* Cooling pumps consumption is not considered.

*All efficiencies are expressed in %.

It can be observed that the power consumption percentage of the fuel cell system auxiliaries remains approximately constant with the current. Considering all the losses (FCS fuel-elec eff.), the fuel cell system efficiency achieved is between 44 and 39% with current densities between 0.4 and 1 A/cm^2 respectively.

FIGURE 4.28: Fuel cell system photo 1

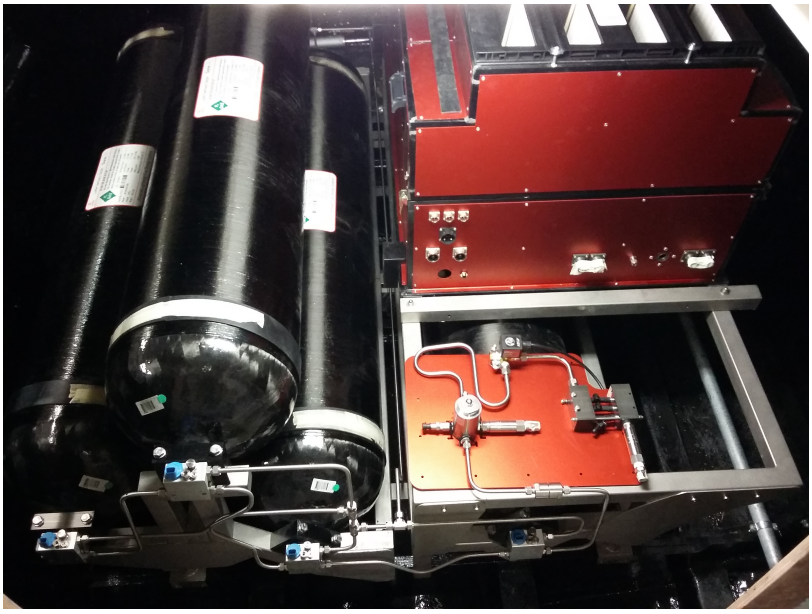

FIGURE 4.29: Fuel cell system photo 2

Chapter 5

Electrical components

5.1 Batteries

They are devices able to store chemical energy and to transform it into electricity and vice-versa. They are one of the core components of hybrid and electric vehicles and, in the last decades, they have attracted the attention of the automotive sector. Just Tesla in the US, in collaboration with Panasonic, is planning to duplicate the world current production capacity of lithium-ion batteries, with its GigaFactory project.

5.1.1 Batteries in the automotive sector

The US Department of Energy and the Advanced Battery Consortium predicted a necessary autonomy of 500km in the electric vehicles to achieve mass-market penetration. Translated into battery requirements, this implies energy densities around 235 Wh/kg and 500 Wh/l at the battery pack level and 350 Wh/kg and 750 Wh/l at the cell level. In addition, the cost needs to fall bellow 125 US$/kWh [32].

Lead-Acid batteries

Invented by Sisteden (1854) and Plantè (1859) [32], they are the oldest and most developed batteries in the automotive sector. They are composed of a sponge metallic lead anode, a lead-dioxide cathode, and a sulfuric acid solution electrolyte.

They are still used in almost all vehicles to power the starter motor, the lights and the ignition system of the vehicle's engine. Despite the fact that they are an economic and already tested technology, they do not fulfill hybrid or electric requirements due to their low energy density. Their energy density is around 40 Wh/Kg and 90 Wh/l and they have Coulombic and energy efficiencies of 80% and 70% respectively [32].

Nickel based batteries

In this category, Ni-cd and Ni-MH are the dominant ones. Considering batteries with the same size, Ni-MH overcomes Ni-cd in terms of power and capacity (30% and 40% improvement respectively) and is more environmentally friendly [36].

Nickel-metal hydride (NiMH) can provide energy densities up to 80 Wh/kg and 250 Wh/l with a nominal voltage of 1.2V [32]. Additionally, they offer high design flexibility (between 30mAh to 250Ah), low maintenance and safe charging and discharging cycles at high voltages. Therefore, they have been widely used in hybrid electric cars such as the Toyota Prius. However, their efficiency is low (70% and 65% of Columbus and energy efficiency respectively [32]) and better energy densities have been achieved in lithium-ion batteries.

Lithium-ion batteries

They are one of the most promising technology and they are becoming dominant in the electric and hybrid vehicles market. They have achieved energy densities around 130-140 Wh/kg and 210 Wh/l with Columbus and energy efficiencies up to 99% and 95% respectively [32]. Additionally, their vast range of power energy ratios makes them adaptable for different applications.

5.1.2 State of the art of lithium-ion batteries

Working principle

These batteries are based on accumulating and liberating chemical energy using lithium. Lithium is unstable in its pure form and has a high tendency to lose electrons. Applying electrical energy, lithium is forced to reach this unstable state accumulating chemical energy. This chemical energy is liberated during the discharge process, in which lithium is forced to feed an electric load to return to its stable state.

The main elements are the separator and electrolyte, the anode and the cathode. The cathode contains the lithium in its stable state, while the anode retains it when it is charged. The separator and the electrolyte, located between the anode and cathode, act as an electronic barrier that stops electrons but allows lithium ions to pass.

When a voltage is applied, the cathode lithium loses its electrons that electrons pass to the anode through the external wiring. The lithium ions are then attracted by the anode negative charge and pass through the separator carried by the electrolyte. In the anode, the lithium ions and the electrons are recombined and contained by the graphite (they do not react with graphite), accumulating chemical energy. If the

voltage source is substituted by an electric load, the discharge process starts. The lithium ions and the electrons dissociate and go back to the cathode to reach a more stable state. When the electrons move back to the cathode, they are forced to pass through the load, providing energy. Finally, the lithium ions, electrons, and the cathode material recombine returning to the initial state.

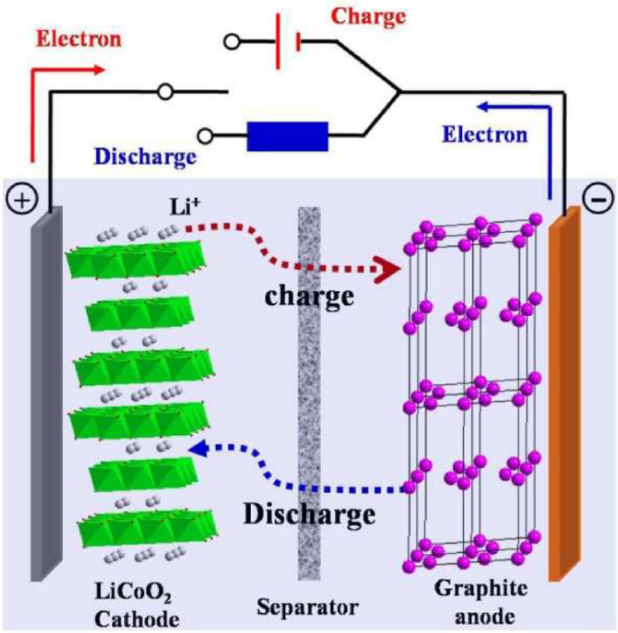

FIGURE 5.1: Lithium battery performance [19]

Anode materials

Graphite is the dominant anode material in lithium-ion batteries. It has an energy density of 372 mAh/g [19], good electrochemical performance and it is widely available and cheap. It has been optimized since it was commercialized twenty years ago, almost reaching its theoretical capacities. Therefore, the expected improvements are limited and some attempts to use metals with higher theoretical energy densities have been carried out. Silicon, with an energy density of 4200mAh/g [19], is the main candidate, however, it expands excessively during charging and discharging. These volume expansions reach values up to 300%, causing damages to the battery and significantly reducing its lifetime. The efforts are now focused on adding only small amounts of these materials so the capacity is increased without damaging the battery.

Some other common anode materials are lithium allowed metals, especially the Li4Ti5O12 (LTO). Excellent stability over time is countered by a higher price and a lower energy density and cell voltage compare to graphite.

TABLE 5.1: Lithium ion batteries: anode materials [19]

Anode Material	**Energy Density (mAh/g)**	**Cost**	**Lifetime**
Graphite	372	Medium	Medium
$Li_4Ti_5O_{12}$ (LTO)	175	High	High

Cathode materials

There is more variety when it comes to select the cathode material. The material is chosen depending on the application requirements in terms of energy density, cost, and life. The most common cathodes materials are shown in table 5.2.

TABLE 5.2: Lithium ion batteries: cathode materials [19]

Cathode Material	**Energy Density (Wh/kg)**	**Cost**	**Lifetime**
$LiCoO_2$ (LCO)	546	Medium	Medium
$LiMn_2O_4$ (LMO)	410–492	Low	Low
$LiNiMnCoO_2$ (NMC)	610–650	High	High
$LiFePO_4$ (LFP)	518–587	Medium	High
$LiNiCoAlO_2$ (NCA)	680–760	High	Medium

LMO, the oldest material in the market, is still common and offers low costs but reduced durability. LCO is another old technology characterized by a medium cost and energy density countered by some safety issues. NMC cathodes are a mix of LMO, LCO and nickel and its properties depend on its mixture proportions. Rich Ni combinations are generally used to increase the cathode energy density. They have attracted the attention of the sector due to their high energy density and lifetime, nevertheless, they are still expensive. LFP is characterized by its extraordinary long term performance and it can be combined with LTO anodes to obtain excellent long term behavior. Finally, NCA cathodes have the highest energy density from the ones presented but they are thermally unstable, which compromises its safety.

Electrolite materials

The electrolyte is made of water with some dissolved salts, generally lithium hexafluorophosphate. If the lithium salts are dissolved in a polymer matrix, batteries are known as lithium polymer batteries.

Examples on the market

From the automotive batteries presented in figure 5.3, the higher cell level energy densities (260 Wh/Kg and 683Wh/l) belong to the model Tesla 3.

TABLE 5.3: Lithium batteries in the automotive sector [32]

Cell format	Cell chemistry		Cell configuration and characteristics				Battery size and range		Cell use
	Anode	Cathode	Capacity (Ah)	Voltage (V)	Specific energy ($Wh\,kg^{-1}$)	Energy density ($Wh\,l^{-1}$)	Energy (kWh)	Driving range (km)	OEM and model[a]
Prismatic cells									
Li Energy Japan	C	LMO-NMC	50	3.70	109	218	16	160	Mitsubishi i-MIEV (2008)
Toshiba	LTO	NMC	20	2.30	89	200	20	130	Honda Fit EV (2013)
Samsung SDI	C	LMO-NMC	63	3.65	172	312	24	140	Fiat 500e (2013)
Samsung SDI	C	LMO-NCA-NMC	60	3.70	122	228	22	130	BMW i3 (2014)
Panasonic/ Sanyo	C	NMC	25	3.70	130	215	24	190	VW e-Golf (2015)
Samsung SDI	C	LMO-NCA-NMC	37	3.70	185	357	36	300	VW e-Golf (2016)
Samsung SDI	C	LMO-NCA-NMC	94	3.70	189	357	33	183	BMW i3 (2017)
Pouch cells									
AESC	C	LMO-NCA	33	3.75	155	309	24	135	Nissan Leaf (2010)
A123	C	LFP	20	3.30	131	247	21	130	Chevrolet Spark EV (2012)
LG Chem	C	LMO-NMC	16	3.70	-	-	35.5	160	Ford Focus EV (2012)
LG Chem	C	LMO-NMC	36	3.75	157	275	26	150	Renault Zoe (2012)
Li-Tec	C	NMC	52	3.65	152	316	17	145	Smart Fortwo EV (2013)
SK Innovation	C	NMC	38	3.70	-	-	27	145	Kia Soul EV (2014)
AESC	C	LMO-NCA	40	3.75	167	375	30	172	Nissan Leaf (2015)
LG Chem	C	NMC	56	3.65	186	393	60	383	Chevrolet Bolt (2016)
LG Chem	C	NMC	59	3.70	241	466	41	400	Renault Zoe (2017)
Cylindrical cells									
Panasonic	C	NCA	3.2	3.60	236	673	60-100	330-500	Tesla S (2012)
Panasonic	Si or SiO–C	NCA	3.4	3.60	236	673	60-100	330-500	Tesla X (2015)
Panasonic	Si–C or SiO_x–C	NCA	4.75	3.60	260	683	75-100	490-630	Tesla 3 (2017)

[a]Year in brackets indicates start of production. C, graphite; Si, silicon; LTO, $Li_4Ti_5O_{12}$; LMO, $LiMn_2O_4$; LFP, $LiFePO_4$; NMC, $LiNi_{1-x-y}Co_xMn_yO_2$; NCA, $LiNi_{0.8}Co_{0.15}Al_{0.05}O_2$; OEM, original equipment manufacturer. Data from refs [4,9] and [82].

Future trends

Higher energy and power densities are required to achieve mass market penetration of electric vehicles. The main paths followed nowadays are:

- Electrodes with higher energy densities
  Some of the possible materials are sulfur (1672 mAh/g), silicon (4200 mAh/g) or lithium metal (3860 mA/g) [19].
- Increase the cell voltage
  The goal is to achieve 5V, a standardized value in electronics
- Develop solid state batteries
  These batteries would get rid of all the safety issues related with electrolyte leakage.

It is extremely complicated to predict batteries long term development, but lithium-magnesium batteries are really promising (high energy density and abundance of materials).

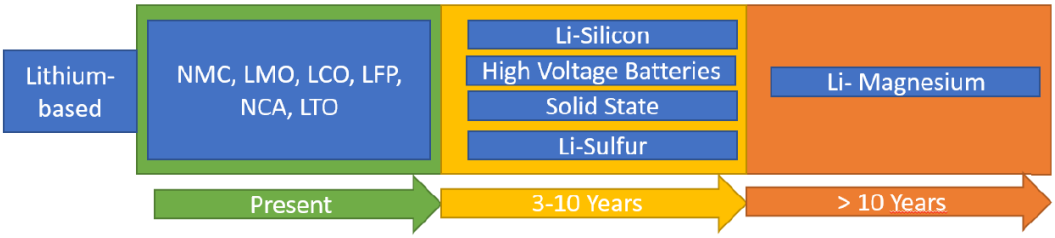

FIGURE 5.2: Future trends of lithium ion batteries [19]

5.1.3 Performance and degradation

The battery voltage varies according to the battery state of charge (SoC); higher SoC values imply higher voltages. During the charging process, the voltage until the maximum voltage is reached. Then the voltage is maintained and current decreases gradually until the battery is completely charged.

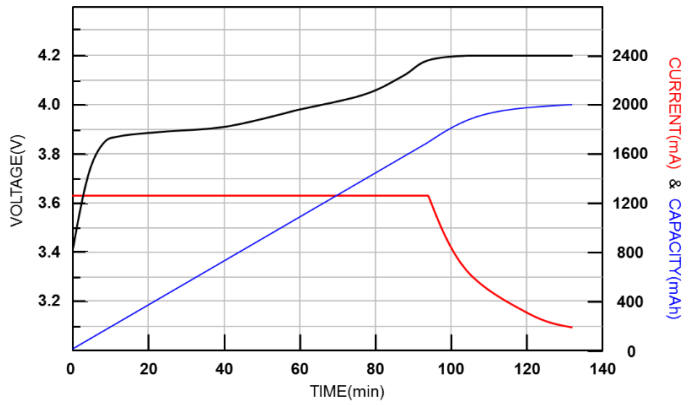

FIGURE 5.3: Generic lithium ion battery charging curve [20]

The battery voltage curve depends on its temperature and current. Lower temperatures or higher currents lead to an increase of the battery internal resistance reducing its output voltage (figure 5.4 and 5.5). The C rate measures the discharge current relative to its maximum capacity; 1C rate indicates that the battery is discharged in one hour, 2C in 30 minutes and 1/2C in 2 hours.

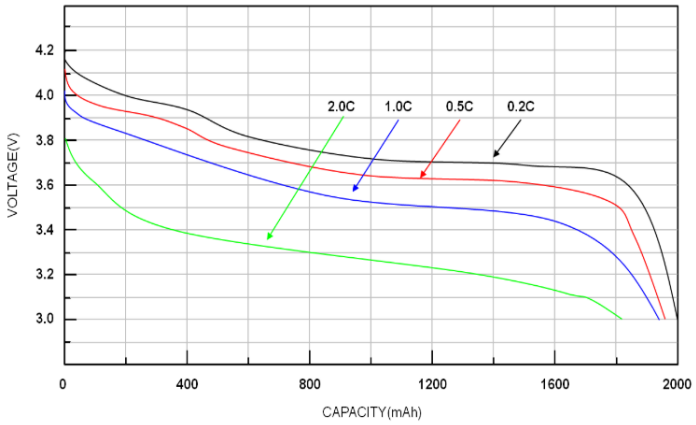

FIGURE 5.4: Current effect on generic lithium ion battery [20]

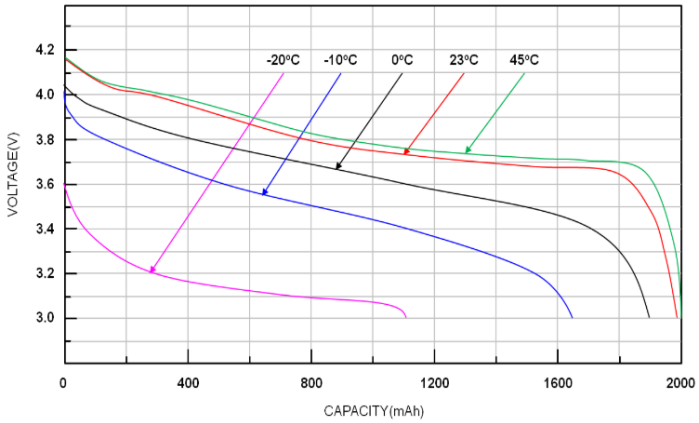

FIGURE 5.5: Temperature effect on generic lithium ion battery [20]

If the battery voltage reaches voltages around 2,5 V, some chemical reactions may occur that damage the battery. In this case, its self-protection generally disconnects them from the circuit. Nevertheless, even if no load is connected, batteries slowly discharge with time. Lithium-ion batteries generally have a self -discharge around a 1 or 2 % percent per month [20]. For these reasons, our batteries are disconnected from the net if their SoC reaches 5%.

Charging and discharging curves change during the time due to degradation, causing a performance reduction (figure 5.6). Degradation varies depending on the materials and the battery conditions; high temperatures, SoC levels, and currents or deep discharge cycles significantly decrease durability. Temperature and SoC should be kept low even when the battery is not operating.

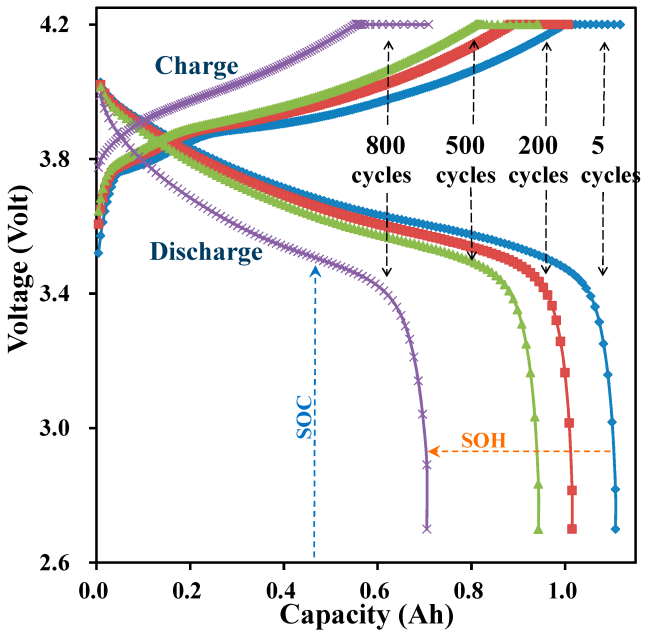

FIGURE 5.6: Lithium ion battery degradation [21]

Modeling degradation is one of the future challenges for lithium-ion batteries and many experiments are currently being carried out. Figure 5.7, obtained from experimental data, shows how battery degradation occurred in a commercial cell with different operating conditions.

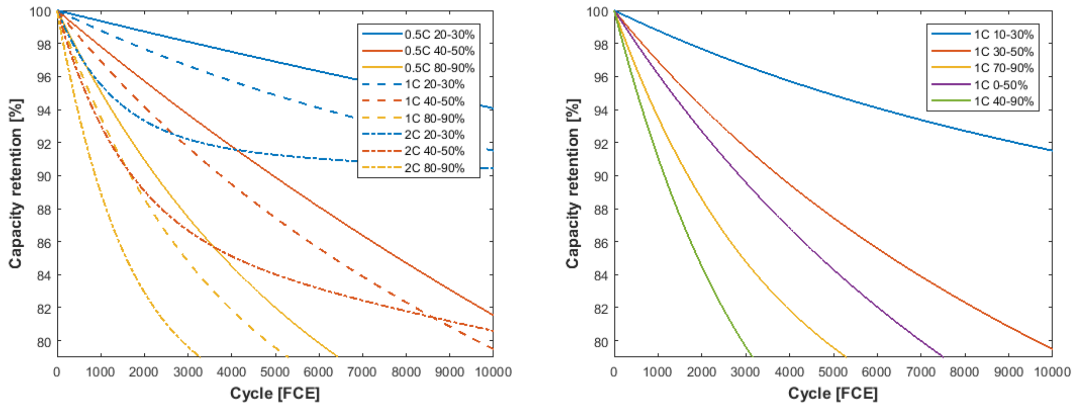

(a) (b)

FIGURE 5.7: Batteries operating parameters and degradation [22]

Selecting a battery with a higher rated power and capacity allows operating with lower values of SoC and C. This should increase its durability and reduce their voltage losses. Therefore, some margin is desired on requirements discussed in section 3.5 if cost, weight and volume available allow it.

5.1.4 Selection

NMC batteries are used in both projects due to their high energy density, however, different models are used in each of the projects. The supplier also provides their complete battery management system (BMS).

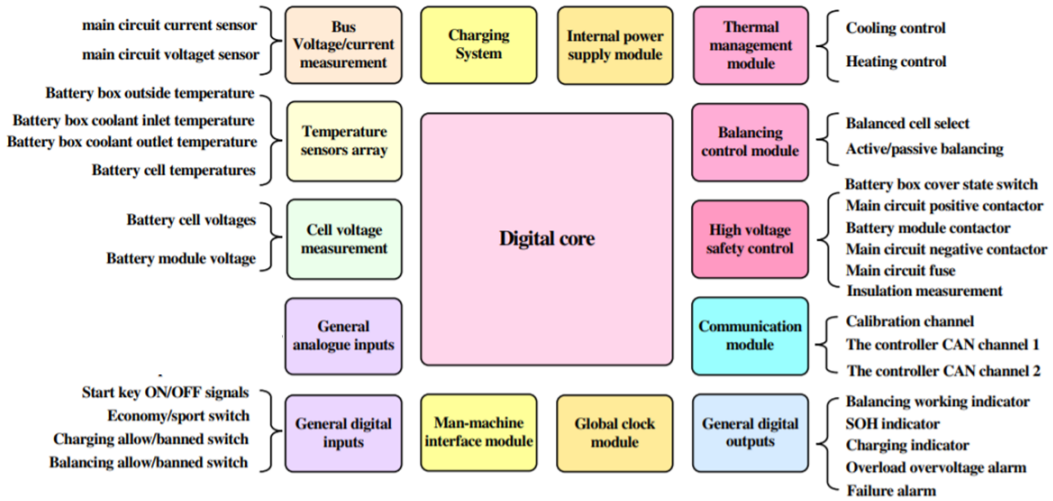

FIGURE 5.8: Generic BMS [23]

Hybrid project

The battery set consists of stacks of lithium-ion NMC batteries connected in series. It has the following overall characteristics:

TABLE 5.4: Battery set hybrid project

Technical characteristics	
Nominal voltage	355 V
Minimum and maximum voltage	307-403 V
Maximum charge current	111 A
Maximum discharge current	120 A
Capacity	111Ah
Available energy	39.42 kWh
Dimensions per stack	0.27 x 1.75 x 0.35 m
Total volume (both stack)	330.75 l
Total weight (both stack)	370 kg

This battery pack can provide continuous discharge currents around 1C with energy densities of 108 Wh/kg and 108 Wh/l and power densities of 113 W/kg and 127 W/l. Figure 5.9 shows their discharge profile with an 80 A current (around 0,7 C) with which they have a nominal power of 28,4 kW.

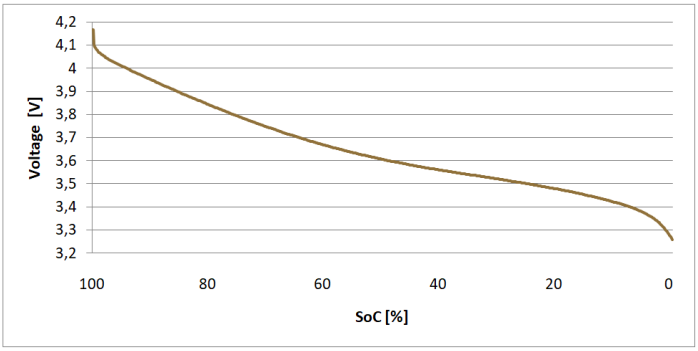

FIGURE 5.9: Discharge profile hybrid project

The battery set only drives the vessel if its SoC is higher than 20%, bellow this value it just feeds the auxiliary electric loads. If its SoC is lower than 5% it is disconnected from the network.

Considering a cell voltage of 3,48 V at a 20% SoC, the minimum voltage and power available in electric mode are 337V and 40,44kW respectively. Therefore, even in the worst condition, there is still a 25% power and current margin. In terms of autonomy, deep of discharge (DoD) cycles lower than 40% can provide the 60 minutes of autonomy desired 3.5.

The battery set is charged with an AC/DC charger that transforms an AC voltage from the grid into a DC one adapted to the batteries. The charger fixes the current around 1/5 C until the maximum voltage is achieved (batteries are charged in 5 hours approximately).

FC project

In this case, power and capacity requirements are significantly higher, while weight and volume constraints remain constant. Higher power and energy densities are required and NMC lithium polymer batteries with high power capacities were selected. A set of 21 stacks joined in a 3x7 structure (three rows of 7 stacks in series connected in parallel) is used. Its global characteristics are:

Table 5.5: Battery set FC project

Technical characteristics	
Nominal voltage	362,6 V
Minimum and maximum voltage	294-408,8 V
Maximum charge current	300 A
Maximum discharge current	900A
Capacity	300 Ah
Available energy	108.8 kWh
Dimensions per stack	0.53x0.21x0.38 m
Total volume (both stack)	888.17 l
Total weight (both stack)	1000 kg

The battery set provides currents up to 3C, achieving power densities of 320W/kg and 361W/l and energy densities of 109 Wh/kg and 123 Wh/l. The discharge profile of a cell with 183,5A is shown in figure 5.10 (in our set this is equivalent to a current of 550A and a nominal power of 200kW).

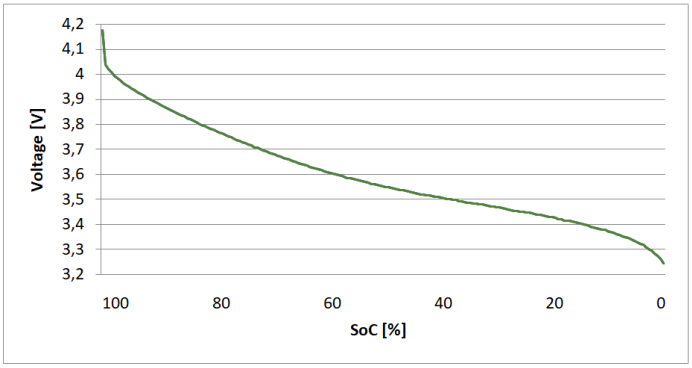

FIGURE 5.10: Discharge profile FC project

The maximum output power of 235 kW is only allowed if the SoC is above 30%, bellow this value it is limited to 120 kW. The vessel can hold its maximum power just for 20 minutes approximately (considering that the batteries are completely charged). Fortunately, in the operating route selected, high power demands are limited to short periods (the high-speed areas last less 10 minutes in a 75 minutes route). If SoC goes go bellow 5% the batteries do not provide more energy and the vessel is powered just with the fuel cell.

Considering a cell voltage of 3,45V at a 30% SoC, the voltage and power are 338V and 304 kW respectively. Even in the worse conditions, there is more than a 50% current and power margin. In terms of autonomy, the energy margin is provided by the fuel cell.

Another AC/DC charger is used, which keeps the current around 1/6 C until the maximum voltage is achieved (the battery set is charged in 6 hours approximately).

5.2 Electric motors

The electric motor is responsible to transform the electrical energy supplied by the batteries into mechanical energy or vice versa (when they work as a generator). A motor controller is needed to adapt the electrical energy coming from the batteries into useful electrical energy for the motor.

5.2.1 State of the art

Motors for vehicle applications are expected to have the following characteristics:

- High torque and power density
- Wide constant power speed range
- High overload capability for transients
- High efficiency in a wide speed and torque range
- Reliability and robustness
- Low noise
- Reasonable cost

In the case of hybrid vehicles is also needed:

- High efficiency as generator
- Facilities to integrate it with the engine

PM synchronous motors and induction motors are the most extended from all the different technologies. While synchronous PM motors achieve higher efficiencies, induction motors have lower prices. The efficiency difference may be especially important when motors operate with partial loads.

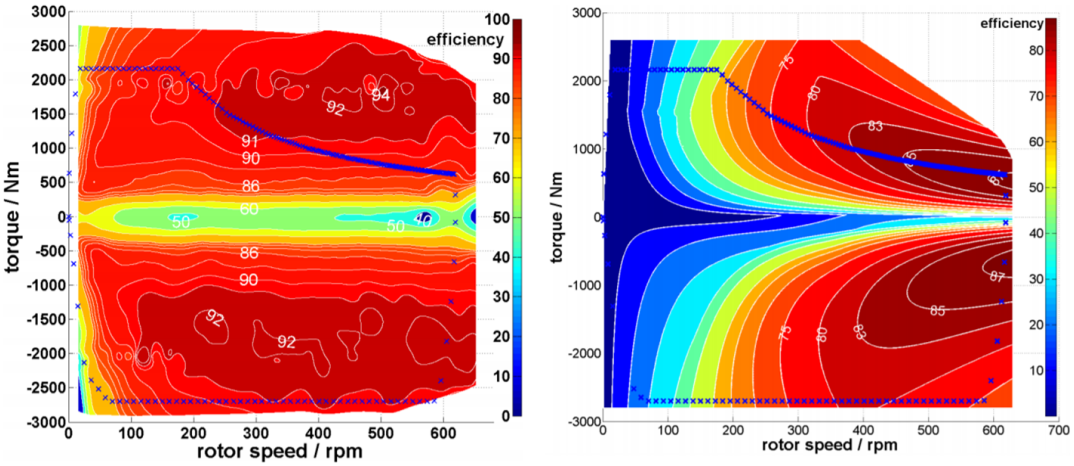

FIGURE 5.11: Efficiency PM synchronous(left) vs induction(right)[24]

TABLE 5.6: State of the art of electric motors

Motor Type	Advantage	Disadvantage	Vehicles Used In
Brushed DC Motor	• Maximum torque at low speed	• Bulky structure • Low efficiency • Heat generation at brushes	Fiat Panda Elettra (Series DC motor), Conceptor G-Van (Separately excited DC motor)
Permanent Magnet Brushless DC Motor (BLDC)	• No rotor copper loss • More efficiency than induction motors • Lighter • Smaller • Better heat dissipation • More reliability • More torque density • More specific power	• Short constant power range • Decreased torque with increase in speed • High cost because of PM	Toyota Prius (2005)
Permanent Magnet Synchronous Motor (PMSM)	• Operable in different speed ranges without using gear systems • Efficient • Compact • Suitable for in-wheel application • High torque even at very low speeds	• Huge iron loss at high speeds during in-wheel operation	Toyota Prius, Nissan Leaf, Soul EV
Induction Motor (IM)	• The most mature commutatorless motor drive system • Can be operated like a separately excited DC motor by employing field orientation control		Tesla Model S, Tesla Model X, Toyota RAV4, GM EV1
Switched Reluctance Motor (SRM) **Synchronous Reluctance Motor (SynRM)**	• Simple and robust construction • Low cost • High speed • Less chance of hazard • Long constant power range • High power density • Robust • Fault tolerant • Efficient • Small	• Very noisy • Low efficiency • Larger and heavier than PM machines • Complex design and control • Problems in controllability and manufacturing • Low power factor	Chloride Lucas
PM assisted Synchronous Reluctance Motor	• Greater power factor than SynRMs • Free from demagnetizing problems observed in IPM		BMW i3
Axial Flux Ironless Permanent Magnet Motor	• No iron used in outer rotor • No stator core • Lightweight • Better power density • Minimized copper loss • Better efficiency • Variable speed machine • Rotor is capable of being fitted to the lateral side of the wheel		Renovo Coupe

Brushed motors suffer from numerous issues and are generally not used anymore in the traction chain. PM brushless DC short constant power speed range is its main problem. Reluctance motors offer a free PM solution with a lower cost but also lower efficiency, torque and power densities. Axial flux ironless PM motors are very promising [37] and may extend in the market in the next years, however, it is still not enough developed.

5.2.2 Selection

PM synchronous motors were selected in both projects due to their high efficiency and torque density and their experience on the market and in previous Dolomitech projects. They are controlled by inverters that transform current from DC to AC three-phase or vice versa. They carry out the internal control,receiving just a speed and maximum current command. Inverter efficiency varies depending on the load (figure 5.12). Motor and controller are acquired as a pack from the supplier with maintenance service included.

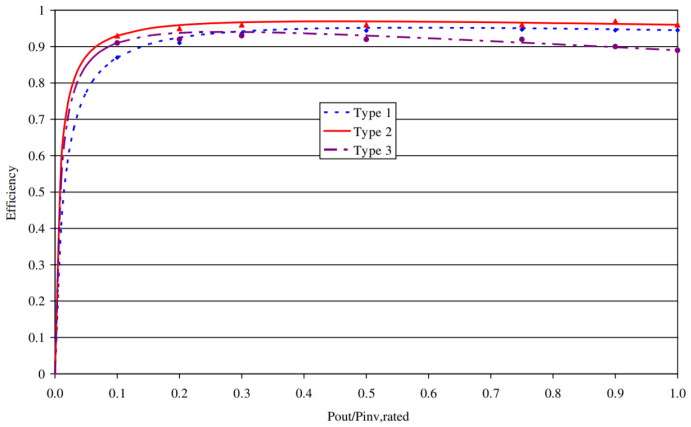

FIGURE 5.12: Generic inverters efficiency vs load[25]

Hybrid project

With the following characteristics, the PM synchronous motor chosen can constantly produce power up to 41 kW.

TABLE 5.7: Electric motor & inverter hybrid project

Technical characteristics	
Nominal current	135 arms
Nominal torque	196.5 Nm
Nominal speed	2000 rpm
Nominal power	41,1kW
Nominal efficiency	92%
Inverter maximum power	90 kW
Inverter peak efficiency	95%

FC project

The PM synchronous motor selected can produce a continuous power of 175 kW and a peak one of 200 kW during 15 minutes.

TABLE 5.8: Electric motor & inverter FC project

Technical characteristics	
Nominal current	
Nominal torque	1100 Nm
Nominal speed	1520 rpm
Nominal power	175 kW
Peak power (15 min)	200 kW
Nominal efficiency	95%
Inverter maximum power	90 kW
Inverter peak efficiency	95%

Instead of one inverter, 3 inverters are used to feed the motor. To make sure that all 3 provide the same amount of power one of them was selected as the master. The master is commanded in speed and it commands the slaves in torque to avoid unbalanced operation and ensure that all of them provide the same power.

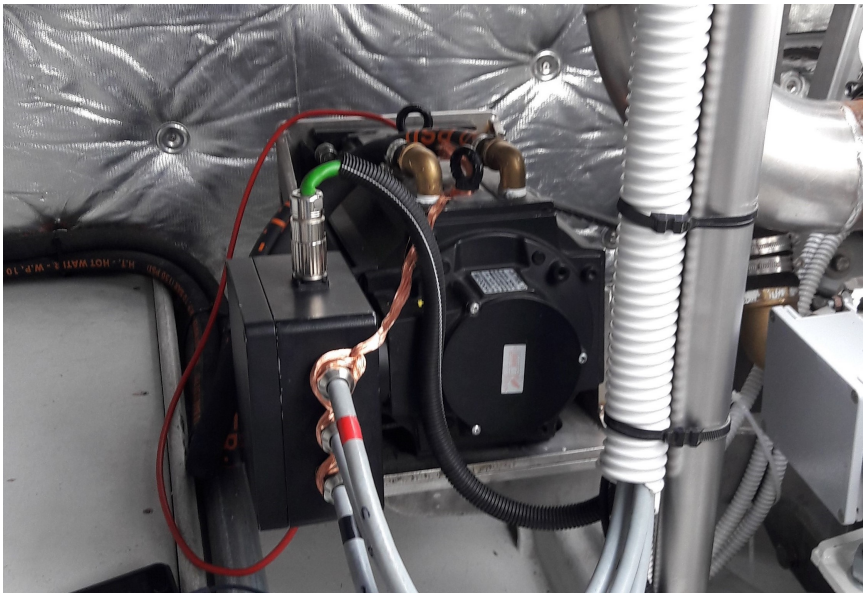

FIGURE 5.13: Hybrid project motor mounted

FIGURE 5.14: FC project inverters and motor during tests

Chapter 6

Thermal design

6.1 Heat estimation

The heat produced can be estimated equal to all the losses (equation 6.1). It is a conservative estimation provides as the components transmit part of the heat to the environment.

$$Q = P_{in} - (1 - \eta) \tag{6.1}$$

The operation parameters of a cooling circuit are related through the following equation:

$$Q = C_p \cdot \dot{m} \cdot (T_{out} - T_{in}) \tag{6.2}$$

where C_p is the coolant specific heat, $\dot{m}$ the coolant mass flow and T_{out} and T_{in} are the coolant output and input temperature in the circuit. Once the maximum power is known (equation 6.1), a maximum temperature interval is established depending on the sensibility to thermal stress. Finally, the maximum flow required is calculated and proper pumps are selected according to the pressure losses.

$$\text{Volumetric flow} = \frac{Q}{C_p \cdot \rho \cdot (T_{out} - T_{in})} \tag{6.3}$$

The unlimited access to seawater makes cooling in vessels significantly simpler compared to road vehicles. Consequently, margins could be easily applied to temperature intervals and pumps and it was not necessary to be extremely precise in the calculations.

6.2 Cooling systems

Each cooling system consists of a heat exchanger and two circuits, an external and an internal one. The internal circuit transmits the thermal power to the external circuit and the external circuit transmits it to the environment. Both circuits are connected through the heat exchanger.

The internal circuit is a closed circuit that connects the different components with one side of the heat exchanger. In the absence of peculiar requirements, the coolant is a combination of water and ethylene glycol. Ethylene glycol reduces the freezing temperature point preventing the water to freeze in winter. However, it reduces the specific heat, resulting in lower thermal capabilities and higher flows. Temperatures in Venice do not reach values under -10ºC so a 25% glycol in volume combination was selected. As the density does not vary significantly, a density of 1kg/l is used for the calculations (6.3).

TABLE 6.1: Water and ethanol glycol combination

% volume glycol	**Freezing temperature**	**Specific heat at 40ºC**
0	0ºC	4,18 kJ/(kgK)
25	-10ºC	3,87 kJ/(kgK)
50	-37ºC	3,4 kJ/(kgK)

The external circuit is an open circuit that introduces seawater in the heat exchange and returns it to the sea at a higher temperature. In this case, the density and specific heat considered were 1kg/l and 4 kJ/(kgK).

Circuit temperatures are controlled by varying the coolant flows. The internal circuits designed to limit the differential temperatures in the components, while the external circuit is used to control the overall temperature. The pumps of the internal circuits are controlled in open-loop according to the vessel operation parameters. In the external circuits, the control is implemented in a closed loop that uses temperature measurements from the internal circuit as feedback.

6.3 Hybrid project

Just the inverter and the electric motor need refrigeration. Under maximum load conditions, the motor and inverter efficiencies were considered 90% and the input power 40kW (maybe more power is used in the future).

$$Q_{inv} = 40 \cdot (1 - 0,90) = 4kW$$
$$Q_{mot} = 36 \cdot (1 - 0,90) = 3,6kW$$
$$Q_{tot} = 4 + 3,6 = 7.6kW \approx 7.5kW$$

There is only one cooling system in the vessel (figure 3.6). In the internal circuit, the inverter and motor are connected in series and the coolant used is a combination of water and ethylene glycol (25% volume ethylene). A temperature interval of 10 ºC is established in both circuits, so the maximum required flows are (equation 6.3):

$$Internal\ flow_{req} = \ External\ flow_{req} \approx \ 12\ l/min$$

The internal pump speed is commanded according to the throttle percentage demanded. The external pump is controlled using the water temperature measured in the motor and inverter (two temperature sensors are situated in their coolant exits). Both pumps have a minimum speed set to ensure that there is always coolant flowing.

6.4 FC project

In this case, several components need refrigeration and the heat generated must be estimated for each component :

- Traction inverters & electric motor.
  The maximum system input power is 200kW, however, it cannot be maintained for long periods. Considering the batteries completely charged, in less than 25 minutes the batteries would reach a 30% SoC and the power would be limited (in reality it will not be kept for more than 5-10 minutes). A power of 140 kW and efficiencies of 93% were considered.

  $$Q_{inv,traz} = 140 \cdot (1 - 0,93) = 9,8kW$$
  $$Q_{mot} = 131,1 \cdot (1 - 0,93) = 9,1kW$$

- DC/DC high voltage.
  The efficiency is around 93% and the maximum operating fuel cell power will not exceed 30kW due to durability issues.

  $$Q_{DC/DC} = 30 \cdot (1 - 0,93) = 2,1kW$$

- Air compressor inverter.
  The maximum input power remains bellow 4kW (for simplicity same value is used for the inverter and compressor). Their efficiencies are around 70% and 90% respectively.

  $Q_{inv,air} = 4 \cdot (1 - 0,7) = 1,2kW$
  $Q_{comp,air} = 4 \cdot (1 - 0,7) = 0,4kW$

- Auxiliary DC/DC converters and hydrogen pump and its inverter.
  Their thermal power is negligible with respect to the other components.

- Fuel cell
  The heat produced has already been modeled in section 4.2.5.

Two cooling systems are needed in the vessel; one refrigerates the fuel cell while the other one cools the rest of components.

6.4.1 Standard cooling system

It is analog to the previous one explained in the hybrid project, however, the high number of components leads to a more complex structure represented in figure 6.1.

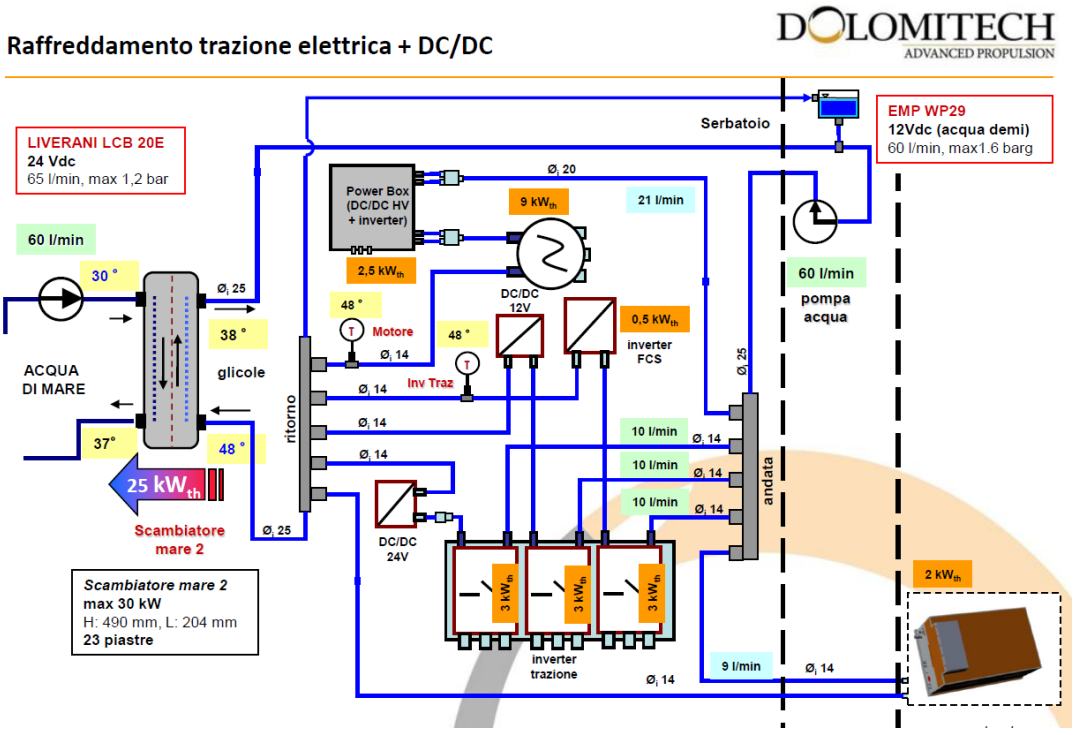

FIGURE 6.1: Standard cooling system

The internal circuit is divided in five branches, which require the following flows:

- Powerbox electric motor
  The powerbox, equipped with a cooling plate, consists of the high voltage DC/DC converter and the hydrogen pump inverter.

  $Q_1 \approx 10.5\ kW$
  $Flow_1 = 16\ l/min$

- Traction inverter auxiliary DC/DC 24V

  $Q_2 \approx 4\ kW$
  $Flow_2 = 6\ l/min$

- Traction inverter auxiliary DC/DC 12V

  $Q_3 \approx 4\ kW$
  $Flow_3 = 6\ l/min$

- Traction inverter inverter compressor FC

  $Q_4 \approx 4\ kW$
  $Flow_4 = 6\ l/min$

- Air compressor hydrogen pump
  The air compressor was designed for another project and its motor operates with fewer margins than normally. As a result, a 3 ^{o}C desired interval was established to reduce its thermal stress and ensure its durability.

  $Q_5 \approx 2\ kW$
  $Flow_5 = 10\ l/min$

Due to its complexity, the maximum external temperature interval is established in 7^{o}C. The whole system is kept colder providing a global margin and reducing the estimations required accuracy. With a total power transmitted of 25kW, the required maximum external flow is:

$$External\ flow_{req} = 53.5\ l/min$$

For simplicity, the same pumps were selected for both cooling systems in the project and they must fulfill both cooling system requirements. While the standard cooling system has stricter external pump requirements, the fuel cell one has stricter internal pump requirements. Using the same pumps simplifies the tests, maintenance and software development and provides extra margin (it can compensate a not uniform flow division in the different branches) .

In this case, different pressure losses tests were performed in order to choose the proper pumps. The ones selected were the EMP and the LCB 20/E models (figures 6.2 and 6.3).

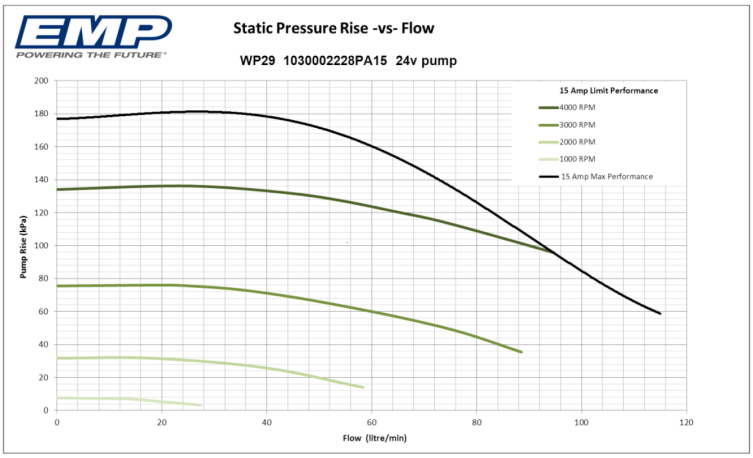

FIGURE 6.2: Internal pumps FC project

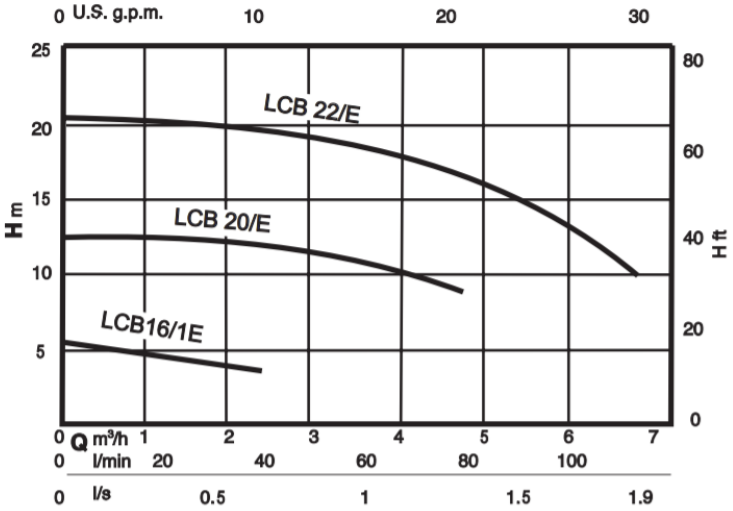

FIGURE 6.3: External pumps FC project (LCB 20/E)

The pump speed control is also analog to the one in the hybrid project, however, the internal pump speed depends not only on the throttle percentage but also on the fuel cell current. With respect to the external pump, water temperature is measured in three components: one of the traction inverters, the motor, and the air compressor.

6.4.2 Fuel cell cooling system

Due to the temperature influence on the fuel cell performance, the desired temperature must be maintained. In addition, the fuel cell requires a different circuit with a coolant conductivity bellow 5 S/c. As a result, the fuel cell has its own cooling system.

The fuel cell is not expected to produce more than 30 kW (300A), so according to section 4.2.5, the heat produced should not exceed 28kW. However, losses may increase due to degradation, and maximum heat of 35 kW is considered. Deionized water is used and a filter system with ion exchange resins keeps it in optimal conditions. Density and specific heat remain practically equal in deionized water.

The Fuel cell is more sensitive to thermal stress than the previous components, so even if 10ºC intervals could be accepted, a 7ºC one is desired. To keep the temperature around 55ºC, a temperature interval of 13 ºC is established for the external circuit. Taking everything into consideration, the maximum required flows are:

Internal flow = 92 l/min
External flow = 40 l/min

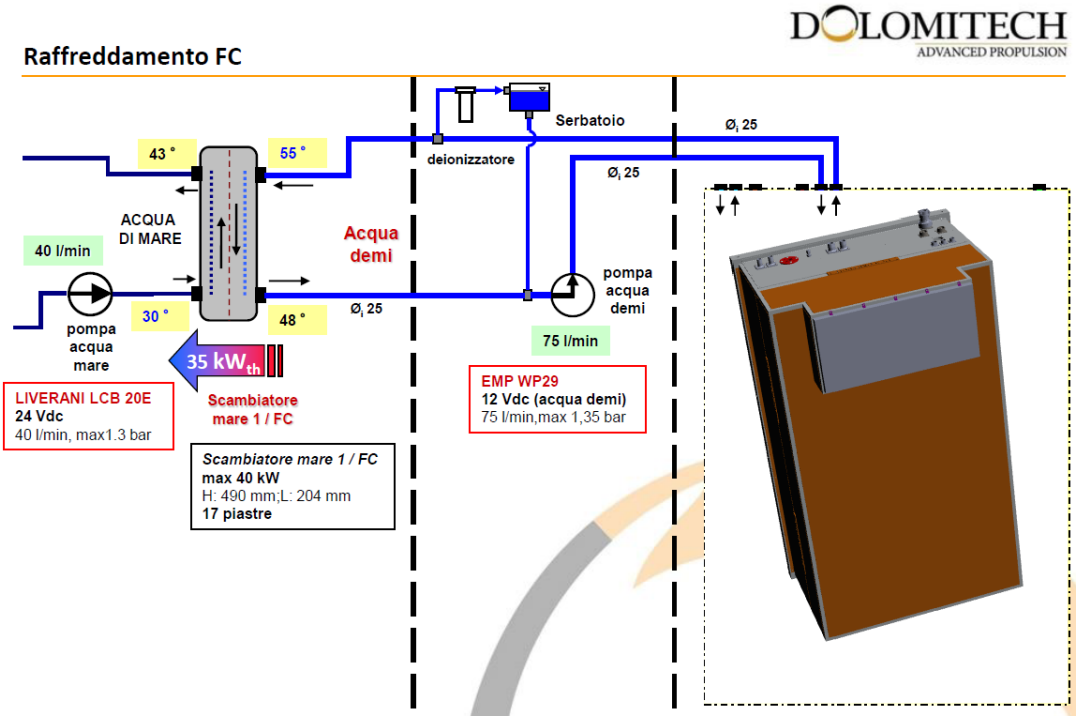

FIGURE 6.4: Fuel cell cooling system

The internal pump speed is commanded in open loop according to the fuel cell current. The external pump is commanded by a proportional controller fed by the temperature error. The fuel temperature is measured in the cathode side and in the coolant exit. Both pumps have a minimum speed set to always ensure coolant flowing.

Chapter 7

Hardware & Software

7.1 Hardware

In both projects, global performance is controlled by an electronic control unit (ECU) designed for the automotive sector. The ECU collects information from sensors, control keys (section 7.1.1) and components to command the different actuators. Its output pins can provide a limited current, so depending on the current demanded, the ECU can supply the actuators directly or through a relay. While CAN networks are used for more complex communications, ECU input pins are used to read sensors and control keys.

7.1.1 Electronic control unit(ECU)

An ECU is an embedded electronic device used in the automotive sector to control one or more systems of the vehicle.

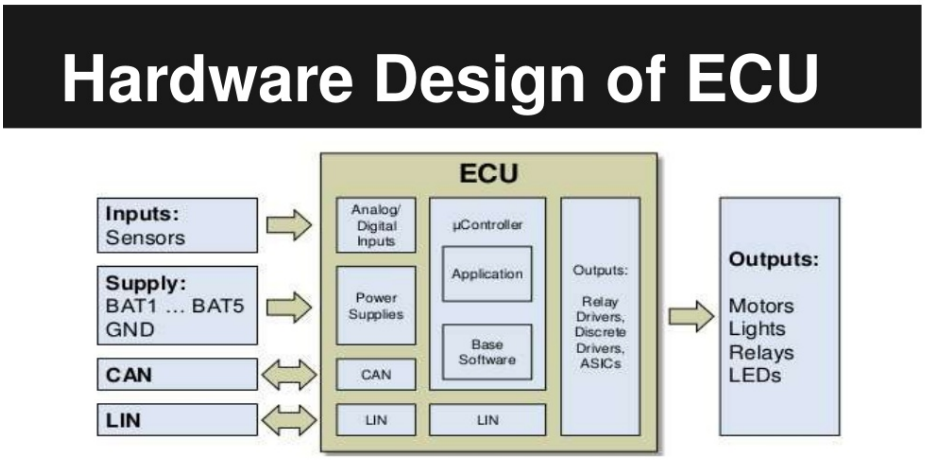

FIGURE 7.1: ECU scheme

The main functional blocks of an ECU are:

- Power supply
  It can provide analog or digital supply to other devices (sensors or actuators)
- Multiple process unit (MPU)
  Microprocessor and memory of the device
- Communication interfaces
  Such as LIN or CAN.
- Digital inputs
- Analog inputs
- Frequency input
- Digital outputs
- Pulse width modulation (PWM) outputs
- Frequency outputs

Inputs: Sensors and control keys

Different sensors are used in the projects to measure the critical operating parameters. They can be classified in the following types:

- Digital Sensors
  - Level sensors
    Located in the deposit of internal cooling circuits, they are used to ensure that there is enough coolant.
  - Limit switches
    A switch is mechanically closed when a component reaches a point. They are used to detect when the batteries charger is connected. In the fuel cell project, they also measure the current state of the air circuit valves.
  - Pressure sensors
    Point out if pressure is higher than a specific value. They reveal possible failures in the hydrogen fuel cell circuit.
  - Switch feedback
    Detect a mismatch between a switch command and its state.

- Analog Sensors
  - Temperature sensors
    Provide information about a component temperature.
  - Pressure sensors
    Measure the hydrogen pressure in different points.
  - Concentration sensors
    They quantify the hydrogen concentration to detect hydrogen leakage.
  - Flow sensors
    Measure the airflow introduced to the air compressor.

We use the term control keys to denote the different digital inputs of the system actuated by the user and used to control the vessel performance.

- Control keys
  - Key
    It turns on the ECU by closing a relay and starts the vehicle turning-on procedure.
  - Emergency bottom
    It is used in case of emergency to stop the vehicle.
  - Diesel off bottom
    It is used in the hybrid project to avoid starting the diesel engine when a high throttle percentage is demanded. However, the engine can still turn on due to electric faults or low SoC values.
  - Fuel cell key
    Turns on the fuel cell.

7.1.2 Hybrid project

ECU

The ECU selected has the following characteristics:

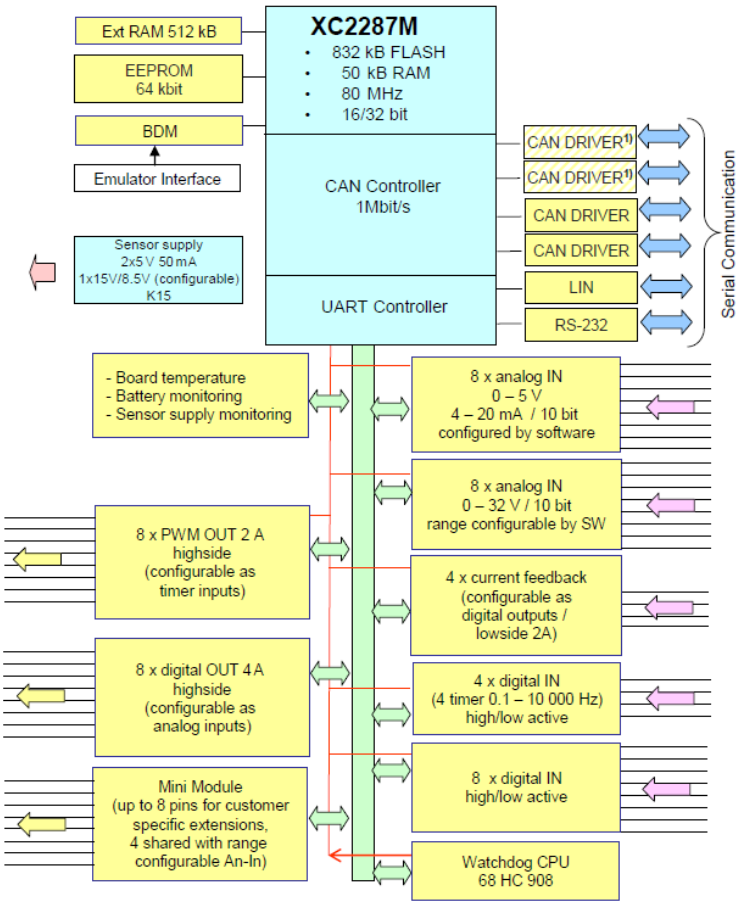

FIGURE 7.2: ECU hybrid project

Input pins

TABLE 7.1: Inputs hybrid project

Control keys	Digital Sensors	Analog sensors
Key	Coolant Level	TempInv_{H_2O}
Emergency	BattCharger	TempMot_{H_2O}
Diesel off		

Output pins

TABLE 7.2: Outputs hybrid project

Digital outputs	**PWM outputs**	
Power BMS	Key Diesel cmd	External pump speed
Power inverter	Cranking cmd	Leds
Power pumps	Forward gear valve	
Precharge contactor	Backward gear valve	
Main contactor	Leds	

7.1.3 Fuel cell project

In this case more pins are needs and the ECU has the following block diagram:

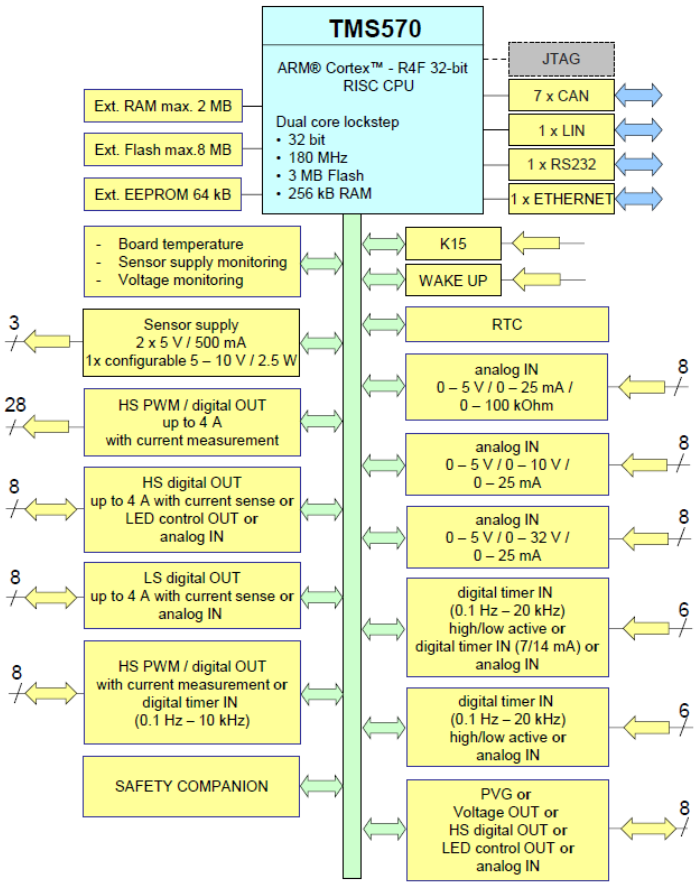

FIGURE 7.3: ECU FC project

Input pins

TABLE 7.3: Inputs FC project

Control keys	**Digital Sensors**	**Analog sensors**	**Analog sensors**
Key	LevelFC	$TempFC_{H_2O}$	TempTank4
Emergency	LevelStd	$TempInv_{H_2O}$	AirFlow
Fuel cell key	In_AirValveOpen	$TempMot_{H_2O}$	H_2Concentration
	In_AirValveClosed	$TempAirComp_{H_2O}$	H_2PressTank
	Out_AirValveOpen	TempAirOut	H_2PressMedium
	Out_AirValveClosed	TempTank1	H_2PressLowIn
	BypassDiode_Feedback	TempTank2	H_2PressLowOut
	OverpressLowOut	TempTank3	
	BattCharger		

Output pins

TABLE 7.4: Outputs FC project

Digital outputs	**Digital outputs**	**PWM outputs**
Power BMS	Power DC/DC 12V	Leds
Power Inverter	Power DC/DC 24V	Speed external pump FC
Power CVM	H_2PressTankValve	Speed internal pump Std
Power DC/DC FC	H_2PressMediumValve	H_2Injector1
Power Display	H_2PurgeValve	H_2Injector2
Precharge contactor	OpenAirValves	H_2Injector3
Main contactor	CloseAirValves	
Power pumps FC	Bypass Diod	
Power pumps Std	Leds	
Power InvCompAir	Buzzer	
InvCompHyd		

7.2 Communication networks

Communications between the global ECU and many of the components take place through CAN networks.

7.2.1 Controller Area Network (CAN)

It is a high-integrity serial network technology designed for vehicles but has been also adopted in the automation industry. Its goal is to allow fast and reliable communication among the different microcontrollers connected to the network. It consists of two shielded or unshielded twisted wires connected to the different nodes or devices. Its maximum signal rate is 1 Mbps with a bus length smaller than 40m and less than 30 nodes [28]. Two en resistors of 120 are used to avoid signal reflection and a transceiver is needed to connect to the network as is shown in figure 7.4.

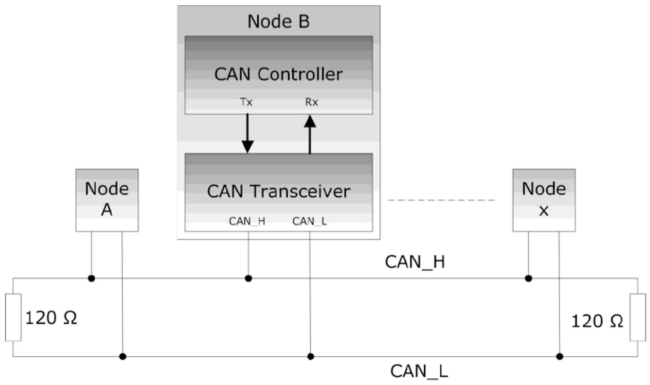

FIGURE 7.4: CAN scheme [26]

Instead of connecting all the different components separately, the components join the network and they can be connected or disconnected without significant network changes. This allows reducing wiring significantly with its consequent cost and weight reduction (figure 7.5). CAN uses a broadcast communication, all the devices can read from the network.

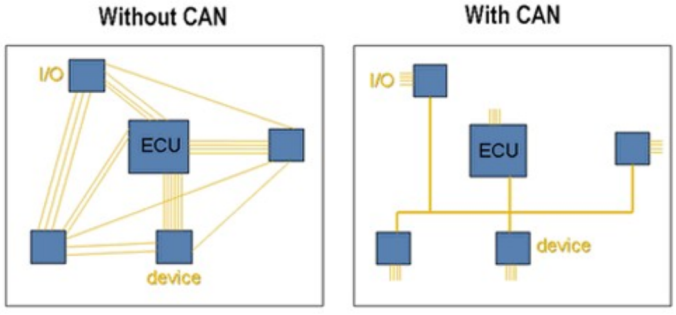

FIGURE 7.5: Weight reduction CAN [27]

CAN uses balance differential voltage to define the signal status. This implies that the same current is passing through both wires but in the opposite direction, resulting in a field-canceling effect. The balance differential voltage combined with twisted pair-cables is the key for common-mode rejection and high noise immunity [28].

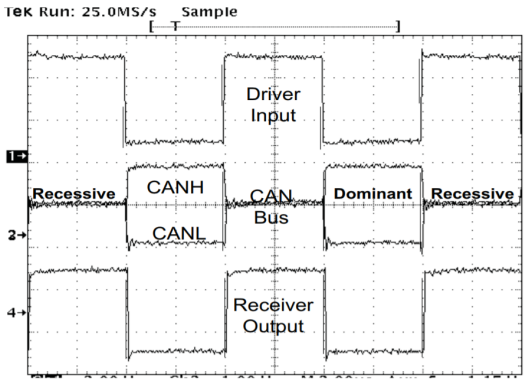

FIGURE 7.6: CAN voltage levels [28]

The network has two different states, the recessive or the dominant state, which correspond to a one and zero respectively. During the recessive state both signals, CAN high (CANH) and CAN low (CANL), are set to 2.5V. On the other hand, in the dominant state CANH increases 1V (3.5V) and CANL decreases 1V (1.5V).

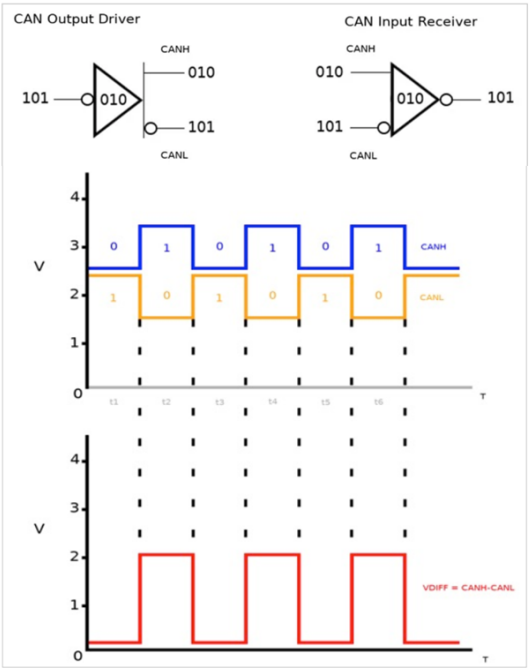

FIGURE 7.7: CAN comunication [29]

CAN uses an inverted logic, which is implemented on the transceivers. It is represented in figure 7.8, where a 101 is transmitted. When a one is transmitted, a zero is sent to CANH and one to CANL creating a differential voltage of OV. To transmit a zero, a one is sent to CANH and a zero to CANL, resulting in a differential voltage of 2V.

All the transceivers contain the information of what they are transmitting and what is the network transmitting, being able to detect mismatches. If two nodes try to write on the bus simultaneously, the dominant state overwrites the recessive one. Both facts are used to avoid message collisions.

When two nodes want to access the bus, the arbitration process starts. Both nodes write on the bus their 11-bit identifier and read the network at the same time. When one of the nodes receives a different bit compared to the one it wrote it backs up. A dominant state always overwrites recessive states, so this can only occur if another node is sending a message with a higher priority (the more zeros the higher is the priority). Therefore, it is a non-destructive arbitration (the winner message continues transmitting without problems). Those messages, which lost the arbitration process, wait until the winning message finishes to attempt again. In figure **??**, node1 and 3 win the arbitration process in the first and second attempts respectively.

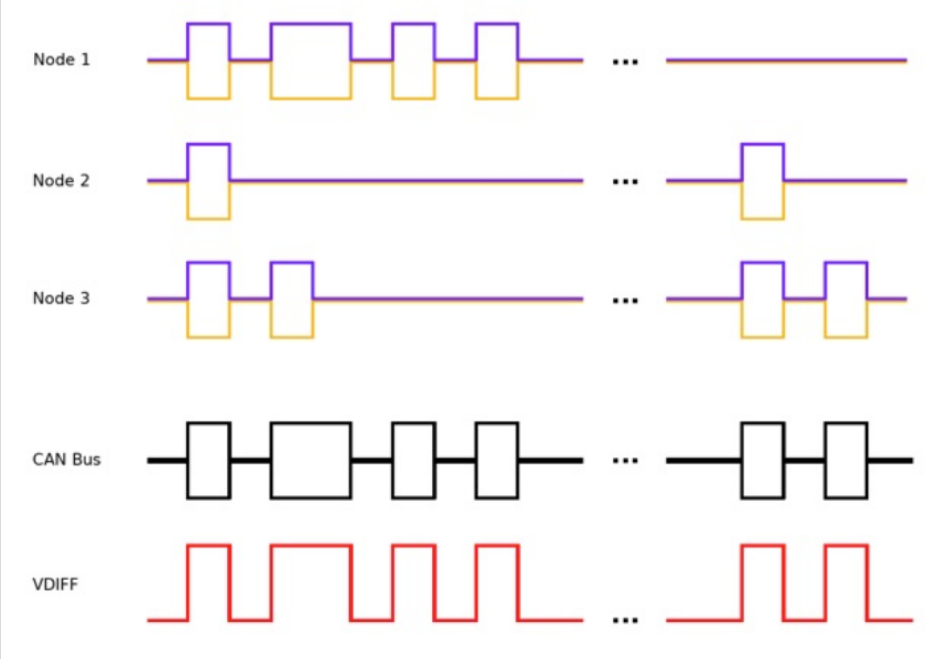

FIGURE 7.8: CAN arbitration [29]

7.2.2 Networks implemented

Hybrid project

Three different CAN networks are used, two of them work at 250 kbps and the other one at 500 kbps. Their combination allows communication along the whole system through the global ECU. Each of them has the following components:

- Global ECU – Diesel engine ECU (250 kbps)
- Global ECU – Display – Throttle - Inverter (250 kbps)
- Global ECU – High Voltage batteries (250 kbps)

FC project

Four CAN networks are implemented, working two of them at 250 kbps and the other two at 500 kbps. They connect the subsequent devices:

- Global ECU – Hydrogen compressor inverter- High Voltage DC/DC - DC/DC 24V - Traction inverters (500 kbps)
- Global ECU - Cell Voltage Monitor- Display (500 kbps)
- Global ECU – High Voltage batteries- Display (250 kbps)
- Global ECU- EMP pumps- Throttle (250 kbps)

7.3 Software

A reliable and robust software has been developed in Codesys to control the performance.

7.3.1 Codesys

The ECU selected accepts two different programming environments, C and Codesys, being this last one the one selected by Dolomitech. Codesys is a development environment for programming controller applications widely used in the sector. It includes the five following programming languages:

- IL (instruction list)
- ST (structured text)
- LD (ladder diagram)
- FBD (function block diagram)
- SFC (sequential function chart)

The code was implemented using ST and SFC, selecting this last one when a graphical interface is desired. Codesys additionally contains a visualization interface that was used to test the code.

With an integrated compiler, the Codesys code was transformed into binary code that can be read by the ECU. Finally, the code is downloaded in the ECU using an application provided by the ECU supplier.

7.3.2 Software development

The software was develooed following the object-oriented programming (OOP) principles to obtain modular reusable software. Just the main functions of each object are described.

- Throttle
  Receive the gear and speed demanded and validate them.
- Pre-charge switches system
  Pre-charge procedure and voltage check.
- Inverter
  Turning on/off procedure and command its speed and maximum current.

- HV batteries
  Turning on/off the BMS and receive information.
- Sensors
  Filter the information and scale it.
- Cooling systems
  Command pumps speed according to different thermal control strategies.
- CAN networks
  Send, receive, and filter information.
- Global diagnostics
  Recognition of performance failures.
- Application
  It is subdivided in different functions. It is responsible of the general application performance.

In the hybrid project, the following objects are added:

- Diesel
  Cranking, synchronization process and gear (valves) control.

In the fuel cell project, the following objects are added:

- Air compressor
  Speed control according to the air flow measured and fuel cell current.
- Hydrogen supply
  Valves control depending on the anode pressure.
- Fuel cell system thermal control
  Pumps speed control and fuel cell current control to keep the desired temperature.
- Power DC/DC converter
  Turning on/off procedure and fuel cell power control.
- Fuel cell system diagnostics
  Detection of failures in the hydrogen part.

Chapter 8

Conclusion & future work

8.1 Current state of the projects

The hybrid project has been finished and it has already been operating for a couple of months. Power and autonomy requirements have been fulfilled and there is still some margin to increase the maximum power of the electric mode. Passengers are especially satisfied with the noise and vibration reduction during its electrical operation and the client with the image improvement.

The fuel cell project has already been constructed and tested but it still has to pass a government certification to be able to carry passengers. However, it has realized a 4h trip between Casale sul Sile and Venezia without issues and power and autonomy requirements are apparently satisfied. The fuel cell operating point may still be modified once its autonomy is tested in real operation. Currently, we are working on the modifications required for this certification that should be passed in the next months.

8.2 Conclusions

Plug-in hybrid powertrains can be an excellent low-emission solution for vehicles that mainly deal with limited operation cycles and load profiles. Electric vehicles operate with zero emissions but have poor autonomy characteristics. More autonomy can be achieved if the system includes a power generation source. While renewable energies such as wind or solar energies have low energy densities and depend on unreliable sources, fuel cells offer a reliable and compact zero-emission generation. Their development may be crucial to complete the expansion of renewable technologies in the transportation sector, especially for heavy vehicles with long operating cycles (trucks, buses, etc...).

Comparing both projects, it was surprising how adding a fuel cell to the system increased exponentially its complexity. Many auxiliary components had to be incorporated and the fuel parameters must be carefully controlled. This complexity increment can be observed in the electric circuits, cooling systems, software codes,

etc... (just the fuel cell system section represents 30% of the thesis). Additionally, the client must find a way to guarantee a hydrogen supply. This results in high operating, designing and production costs that could be reduced by mass production, especially the designing ones.

On the other hand, the fuel cells have a significantly higher energy density. With a similar weight, actually even lower, the fuel cell system can provide more than three times battery set capacity. Just an electric powertrain probably would not be able to satisfy the requirements and weight constrains.

The vessel autonomy allows it to operate with zero emissions, achieving the main goal of renewable vehicles and making it unique.The electric operation implies a significant comfort improvement highly appreciated by the users due to the noise and vibration reduction. Furthermore, it offers a great opportunity to improve the company image and acquire knowledge of this technology that may become fundamental in the future.

These projects expect to encourage the expansion of renewable vehicles to small marine boats. Technology is already prepared to satisfy the small boat requirements and excellent results can be obtained. Nonetheless, more government investments are needed, especially to develop a proper supply infrastructure for hydrogen vehicles.

8.3 Future work

Generating electricity with the diesel engine or the fuel cell is way less efficient than storing it from the grid. To reduce the electric dependency on the sources the following paths will be followed in the future:

- Increase the batteries capacity
  Adding batteries increases the electric energy stored at night.
- Adding charging spots in the route
  Would allow charging the vessel in the last route stops.
- Adding a fast charging
  Especially important for the short charges in the route stops.

In the fuel cell model, the client must develop and hydrogen supply infrastructure to efficiently supply the vessel. Additionally, fuel cell durability and performance will be studied to reduce the margins and project costs for future models.

Bibliography

[1] Eleftherios K Dedes, Dominic A Hudson, and Stephen R Turnock. Assessing the potential of hybrid energy technology to reduce exhaust emissions from global shipping. *Energy policy*, 40:204–218, 2012.

[2] Ameen M Bassam, Alexander B Phillips, Stephen R Turnock, and Philip A Wilson. An improved energy management strategy for a hybrid fuel cell/battery passenger vessel. *International Journal of Hydrogen Energy*, 41(47):22453–22464, 2016.

[3] Nova Scotia Boatbuilders Association. Review of all-electric and hybrid-electric propulsion technology for small vessels, 2015.

[4] N Bennabi, JF Charpentier, H Menana, JY Billard, and P Genet. Hybrid propulsion systems for small ships: Context and challenges. In *2016 XXII International Conference on Electrical Machines (ICEM)*, pages 2948–2954. IEEE, 2016.

[5] Aspin Kemp Associates. http://www.aka-group.com/marine-power/xeropoint-hybrid-propulsion/, 5th of July of 2019.

[6] Foss Maritime. Foss maritime green assist^{TM} hybrid tugboat, 2011.

[7] Electrovaya. Scandinavia's first lithium battery electric car ferry completes six months of winter operations in the norwegian fjords, 2014.

[8] Comune di Venezia. http://www2.comune.venezia.it/motondoso/piantina.pdf, 15th of July of 2019.

[9] Leon F Osborne, Jeff Brummond, Robert Hart, Mohsen Zarean, Steven M Conger, et al. Clarus: Concept of operations. Technical report, United States. Federal Highway Administration, 2005.

[10] Tatsuo Takaishi, Akira Numata, Ryouji Nakano, and Katsuhiko Sakaguchi. Approach to high efficiency diesel and gas engines. *Mitsubishi Heavy Industries Review*, 45(1):21–24, 2008.

[11] https://x-engineer.org/automotive-engineering/internal-combustion-engines/performance/brake-specific-fuel-consumption-bsfc/, 20th of July of 2019.

[12] Vipin Das, Sanjeevikumar Padmanaban, Karthikeyan Venkitusamy, Rajasekar Selvamuthukumaran, Frede Blaabjerg, and Pierluigi Siano. Recent advances and

challenges of fuel cell based power system architectures and control–a review. *Renewable and Sustainable Energy Reviews*, 73:10–18, 2017.

[13] Michael W Ellis, Michael R Von Spakovsky, and Douglas J Nelson. Fuel cell systems: efficient, flexible energy conversion for the 21st century. *Proceedings of the IEEE*, 89(12):1808–1818, 2001.

[14] Abed Alaswad, Ahmad Baroutaji, Hussam Achour, James Carton, Ahmed Al Makky, and Abdul-Ghani Olabi. Developments in fuel cell technologies in the transport sector. *International Journal of Hydrogen Energy*, 41(37):16499–16508, 2016.

[15] Omar Z Sharaf and Mehmet F Orhan. An overview of fuel cell technology: Fundamentals and applications. *Renewable and sustainable energy reviews*, 32:810–853, 2014.

[16] Z Belkhiri, M Zeroual, H Ben Moussa, and B Zitouni. Effect of temperature and water content on the performance of pem fuel cell. *Revue des Energies Renouvelables*, 14(1):121–130, 2011.

[17] Dr. Colleen Spiegel. https://www.fuelcellstore.com/blog-section/fuel-cell-heat-flow, 27th of July of 2019.

[18] Mike Steilen and Ludwig Jörissen. Hydrogen conversion into electricity and thermal energy by fuel cells: Use of h2-systems and batteries. In *Electrochemical Energy Storage for Renewable Sources and Grid Balancing*, pages 143–158. Elsevier, 2015.

[19] Gert Berckmans, Maarten Messagie, Jelle Smekens, Noshin Omar, Lieselot Vanhaverbeke, and Joeri Van Mierlo. Cost projection of state of the art lithium-ion batteries for electric vehicles up to 2030. *Energies*, 10(9):1314, 2017.

[20] https://www.richtek.com/design%20support/technical%20document/an024, 27th of May of 2019.

[21] Shyh-Chin Huang, Kuo-Hsin Tseng, Jin-Wei Liang, Chung-Liang Chang, and Michael Pecht. An online soc and soh estimation model for lithium-ion batteries. *Energies*, 10(4):512, 2017.

[22] Evelina Wikner and Torbjörn Thiringer. Extending battery lifetime by avoiding high soc. *Applied Sciences*, 8(10):1825, 2018.

[23] Languang Lu, Xuebing Han, Jianqiu Li, Jianfeng Hua, and Minggao Ouyang. A review on the key issues for lithium-ion battery management in electric vehicles. *Journal of power sources*, 226:272–288, 2013.

[24] Florian Demmelmayr, Markus Troyer, and Manfred Schroedl. Advantages of pm-machines compared to induction machines in terms of efficiency and sensorless

control in traction applications. In *IECON 2011-37th Annual Conference of the IEEE Industrial Electronics Society*, pages 2762–2768. IEEE, 2011.

[25] Gilles Notton, V Lazarov, and L Stoyanov. Optimal sizing of a grid-connected pv system for various pv module technologies and inclinations, inverter efficiency characteristics and locations. *Renewable Energy*, 35(2):541–554, 2010.

[26] https://copperhilltech.com/a-brief-introduction-to-controller-area-network/, 15th of August of 2019.

[27] https://www.ni.com/en-my/innovations/white-papers/06/controller-area-network–can–overview.html, 10th of August of 2019.

[28] Texas Instruments. Introduction to the controller area network (can). *SLOA101A. Dallas, TX*, 2008.

[29] https://www.allaboutcircuits.com/technical-articles/introduction-to-can-controller-area-network/, 11th of August of 2019.

[30] Himadry Shekhar Das, Chee Wei Tan, and AHM Yatim. Fuel cell hybrid electric vehicles: A review on power conditioning units and topologies. *Renewable and Sustainable Energy Reviews*, 76:268–291, 2017.

[31] Alexander Kabza. Fuel cell formulary. *Alexander Kabza. Recuperado a partir de www. kabza. de*, 2015.

[32] Richard Schmuch, Ralf Wagner, Gerhard Hörpel, Tobias Placke, and Martin Winter. Performance and cost of materials for lithium-based rechargeable automotive batteries. *Nature Energy*, 3(4):267, 2018.

[33] Foss Maritime. https://www.foss.com/press-releases/worlds-first-hybrid-tug-even-greener-than-initial-estimates/, 6th of July of 2019.

[34] Øyvind Notland Smogeli. Control of marine propellers: from normal to extreme conditions. *Fakultet for ingeniørvitenskap og teknologi*, 2006.

[35] Mark AJ Cropper, Stefan Geiger, and David M Jollie. Fuel cells: a survey of current developments. *Journal of Power Sources*, 131(1-2):57–61, 2004.

[36] TMI Mahlia, TJ Saktisahdan, A Jannifar, MH Hasan, and HSC Matseelar. A review of available methods and development on energy storage; technology update. *Renewable and Sustainable Energy Reviews*, 33:532–545, 2014.

[37] Fuad Un-Noor, Sanjeevikumar Padmanaban, Lucian Mihet-Popa, Mohammad Mollah, and Eklas Hossain. A comprehensive study of key electric vehicle (ev) components, technologies, challenges, impacts, and future direction of development. *Energies*, 10(8):1217, 2017.